Review

A Review of 3-D Printing Batteries

Maryam Mottaghi and Joshua M. Pearce *

Posted Date: 14 February 2024

doi: 10.20944/preprints202402.0784.v1

Keywords: 3-D printing; Additive Manufacturing; Batteries; Electricity; Energy; Energy storage; Open source; Open source hardware

Review

A Review of 3-D Printing Batteries

Maryam Mottaghi [1] and Joshua M. Pearce [2,*]

[1] Department of Mechanical and Materials Engineering, Western University, London, Canada; mmottagh@uwo.ca
[2] Department of Electrical and Computer Engineering, Ivey Business School, Western University, London, Canada; joshua.pearce@uwo.ca
* Correspondence: joshua.pearce@uwo.ca

Abstract: To stabilize the Earth's climate a large-scale transition is needed to non-carbon emitting renewable energy technologies like wind and solar energy. Although these renewable energy sources are now lower-cost than fossil fuels, their inherent intermittency make them unable to supply a constant load without storage. To address these challenges rechargeable electric batteries are currently the most promising option; however, their high capital costs limit current deployment velocities. To both reduce the cost as well as improve performance 3D printing technology has emerged as a promising solution. This literature review provides the state-of-the-art enhancements of battery properties with 3D printing including efficiency, mechanical stability, energy and power density, customizability and sizing, production process efficiency, material conservation and environmental sustainability as well as the progress in solid-state batteries. The principles, advantages, limitations, and recent advancements associated with the most common types of 3D printing are reviewed focusing on their contributions to the battery field. 3D printing batteries offer design flexibility, material flexibility, reduces pack weight, minimizes material waste, increases the range of applications and has the potential to reduce costs. As 3D printing technologies become more accessible, the prospect of cost-effective production for customized batteries is extremely promising.

Keywords: 3-D printing; additive manufacturing; batteries; electricity; energy; energy storage; open source; open source hardware

1. Introduction

Global climate change, caused by greenhouse gas emissions from conventional power generation from coal, natural gas, and oil, contributing 18%, 40%, and 1% to global electricity production in 2022, poses a concern [1]. This increases negative impacts on human health [2–4], reduction in agricultural productivity [5], and has economic [6–8] consequences. One approach to eliminating the need for fossil fuel electric generation is to replace it with renewable sources to address these challenges [9]. Among the array of renewable energy (RE) options, wind and solar energy are among the most important ones due to their widespread availability and abundance [10]. Although these RE sources contributed approximately 11.88% to global energy production in 2022, predictions indicate they could supply up to 50% of the world electricity demand by 2050 [11,12]. Nonetheless, the inherent intermittency and variability of wind and solar resources make them unable to supply a constant load without storage [13–19]. To address these challenges, various energy storage solutions have been explored, with rechargeable electric batteries emerging as a highly promising option [20]. In addition, with the record growth of electric vehicle (EV) there is a potential for EV charging to add to stability with a high penetration level RE grid [21]. One of the drawbacks of rechargeable electric batteries is their high cost and a crucial factor influencing battery production costs is the manufacturing process [22]. In this context, 3D printing technology has emerged as a promising solution to address cost concerns associated with battery production, offering a layer-by-layer approach, which has already been shown to reduce costs for a wide array of products including

 doi:10.20944/preprints202402.0784.v1

those used to do battery research such as an open-source ball mill [23], open source bottle roller [24], sample shaker [25], sample stirrer [26], and numerous additional broader applications [27–29]. Utilizing 3D printing in battery fabrication enhances performance, increases design flexibility, reduces pack weight, minimizes material waste, and shortens production time, ultimately leading to cost reductions [30,31]. Recognizing the enormous potential significance of 3D printing in battery production, this paper provides a detailed review of the most promising 3D printing methods employed in this context. First to provide background the types and geometries of batteries will be summarized. Then the literature will be reviewed focused on enhancing battery properties with 3D printing including: efficiency, mechanical stability, energy and power density, customizability and sizing, production process efficiency, material conservation and environmental sustainability and solid-state batteries. Finally, the principles, advantages, limitations, and recent advancements associated with most common types of 3D printing (direct ink writing (DIW), fused filament fabrication (FFF), inkjet printing (IJP), and stereolithography (SLA)) will be reviewed focusing on their contributions to the field of energy storage. This work will be synthesized, discussed and conclusions will be drawn about the impact of 3D printing on the electric battery technologies able to back up intermittent renewable energy for the future of a sustainable electric system.

2. Background

2.1. Battery basics

2.1.1. Energy

Energy density is the amount of energy stored in a given volume or mass which defines the battery capacity. The specific energy density or the gravimetric energy density is the energy in the specific weight measured in Wh/kg and the volumetric energy density is the energy stored in the specific volume measured in Wh/m^3.

2.1.2. Power

Power density is the rate that the energy is transferred within the battery structure that is particularly crucial in applications such as electric vehicles, where rapid energy delivery is required. Specific power density refers to the rate at which a battery can deliver electrical power relative to its weight and quantifies how quickly a battery can discharge its stored energy, typically measured in watts per unit of weight (W/kg). Volumetric power density signifies the rate at which a battery can deliver electrical power relative to its volume and is measured in watts per unit of volume (W/m^3).

2.1.3. Voltage

Nominal voltage indicates the average voltage value assigned to a particular type or model of battery for design and specification purposes. It is often used as a reference point and does not reflect the actual voltage of the battery at any specific moment during its operation. Open circuit voltage (OCV or V_{OC}) is the voltage across the battery terminals when no current is flowing. It represents the potential difference between the positive and negative terminals in the absence of a load and is an indicator of the SOC.

2.1.4. State of the charge (SOC)

SOC is the amount of energy stored in a battery at a given moment and is expressed as a percentage (%) of the total capacity. It indicates how much charge is available for use.

2.1.5. Capacity

Total capacity represents the maximum number of ampere-hours that can be extracted from a fully charged battery cell before it is fully discharged. This limit is determined by the SOC and involves discharging from 100% to 0%. Discharge capacity is the quantity of ampere-hours that can

 doi:10.20944/preprints202402.0784.v1

be drawn from a fully charged cell at a constant current rate, stopping before encountering a minimum voltage limit. Unlike total capacity, it does not indicate the complete charge a cell can hold, as it discharges from 100% to a minimum voltage. Reversible charge capacity refers to the amount of charge that can be cyclically stored and released in a reversible electrochemical reaction and indicates the stability of the electrochemical process.

2.1.6. Voltage drops

There are several potential mechanisms that result in voltage drops. First, activation loss happens due to the slow nature of the reactions that occur on the electrode surface. Fuel crossover and internal currents result from electrons passing through the electrolyte which leads to the charge loss in this way. Ohmic loss, or internal resistance, is the energy loss resulting from resistance to the flow of electrons through electrode materials and interconnections, as well as resistance to the flow of ions through the electrolyte. Mass transport (concentration) loss occurs when the electrode surface is depleted from charges over time, and reactants require time to diffuse from the inner bulk to the surface for the reaction to keep on.

2.1.7. Self-discharge

Self-discharge is the result of unwanted chemical reactions that occur internally, leading to various issues such as current leakage, dendrite formation, electrolyte decomposition, and electrode decomposition. These processes contribute to the gradual discharge of a battery even when it is not in use.

2.1.8. Electrical double layer

During battery operation, the charged electrodes interface with the electrolyte result in the formation of a layer of charges. This occurs due to the attractive forces between the charged electrode surface and the ions present in the electrolyte, and it is referred to as the electrical double layer.

2.1.9. Lithiation/ Delithiation

Lithiation describes the insertion of lithium ions into anode and delithiation refers to the removal from the anode during the charging and discharging of a lithium-ion battery, respectively.

2.1.10. Particle pulverization

Particle pulverization in lithium-ion batteries refers to the mechanical fragmentation or disintegration of electrode materials, especially in the anode, as a result of repeated cycles of lithium-ion intercalation and deintercalation during charging and discharging.

2.1.11. Lithium plating

When the battery voltage exceeds a certain threshold during charging, the excess voltage drives the reduction of lithium ions at the anode surface, leading to the deposition of metallic lithium which is more likely to occur at low temperatures; lower temperatures reduce the lithium-ion mobility and make it easier for lithium ions to deposit as solid lithium on the anode surface which is called lithium plating.

2.1.12. Solid electrolyte interface

During the initial cycle, the electrolyte containing lithium salt decomposes to create reactive species. These reactive species, along with the lithium ions, precipitate on the anode surface. This ongoing process results in the formation of multiple layers with different chemical compositions and properties. Maintaining an optimum thickness in this layer is crucial as it can provide mechanical stability and prevent further decomposition. It is essential, however, for this layer to be thin enough not to reduce ionic conductivity.

 doi:10.20944/preprints202402.0784.v1

2.1.13. Charge/discharge test

The charge/discharge test involves applying a constant current while considering the cut-off voltage and scan rate. During charging, the constant current leads to an increase in potential until the cut-off voltage is reached. Then, the current is reversed, and the potential starts to decrease to the minimum cut-off voltage. This test is a fundamental method for evaluating the capacity, reversibility, stability, and rate capability of the battery.

2.1.14. Cyclic voltammetry test

This test involves tracking the current by linearly sweeping the voltage over time with a specified scan rate, which is higher than that used in charge/discharge cycles. The reason for this is that the test is employed to study the redox reactions, reaction kinetics, and electrochemical behavior of the materials within the battery.

2.1.15. Electrochemical Impedance Spectroscopy (EIS)

EIS is a test that measures various impedance elements in a battery system by applying a small alternating current across a wide range of frequencies and measuring the corresponding response. The output of the test is a plot called Nyquist plot which is made of the real part the impedance on the x axis and the imaginary part of the impedance on the y axis. An equivalent circuit is constructed from a Nyquist plot in order to model and analyze the electrochemical behavior of a system. Different parts of the curve can be explained as the following:

- Ohmic resistance (Rs) is related to the ionic and electronic conductivity of various components in the battery, including the electrolyte, electrodes, and current collector. This is measured at low frequencies, and on the Nyquist plot, it is represented by the real part of the impedance (Figure 1a).
- Charge transfer resistance (Rct) is the resistance related to the electrochemical reactions occurring at the interface layer of the electrode-electrolyte. Information about the kinetics of the charge transfer process, such as lithium intercalation at the electrode surface, is provided by this resistance. On the Nyquist plot, this resistance is observed as a semicircle, with the radius of the semicircle representing the charge transfer resistance. This region corresponds to the high-frequency range. An improvement in battery performance is indicated by a reduction in the radius/diameter of this semicircle, suggesting that the charge transfer processes at the electrode-electrolyte interface are more efficient and faster. This layer also serves as a capacitance that stores charges transferring slowly to the electrode. In the equivalent circuit, it is represented as a capacitance in parallel to the charge transfer resistance (Figure 1b).
- Warburg impedance (W) is related to the diffusion (mass transport) of lithium ions into the solid electrode and electrolyte. On the Nyquist plot, it is represented by a sloped line. This region corresponds to the medium frequency range on the plot. The slope of the line reflects the diffusion coefficient of the species. A steeper slope indicates more difficult ion diffusion, while a shallower slope suggests easier mass transport and diffusion. The tail of this impedance is also significant. Tail extensions or deviations from the line indicate additional electrochemical processes occurring in the battery (Figure 1c).

 doi:10.20944/preprints202402.0784.v1

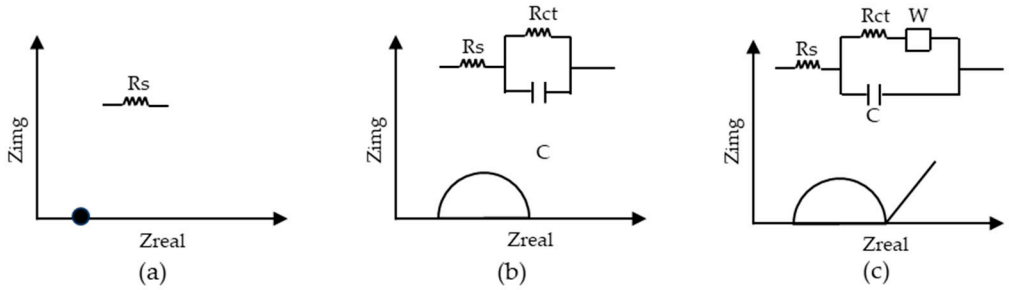

Figure 1. Nyquist plot, (a) Ohmic resistance, (b) Charge transfer resistance, and (c) Warburg resistance.

2.2. Basic types of batteries

In general, batteries are divided into two categories; primary and secondary batteries [32]. Primary batteries, also known as disposable or non-rechargeable batteries, are designed for single-use applications. They provide a reliable source of power by converting chemical energy into electrical energy. Common examples include zinc–carbon, alkaline zinc–manganese dioxide, and metal–air- batteries [33]. Primary batteries are used for low and intermittent power needs, such as remote controls and smoke detectors [34]. They are however, one of the most expensive sources of electric energy and in general should be replaced by secondary batteries [35]. Secondary batteries are rechargeable batteries that can be reused multiple times by reversing the chemical reactions through an external power source, like a charger. Popular secondary battery types include lead acid, nickel-cadmium (NiCd), nickel-metal hydride (Ni-MH), and lithium-ion (Li-ion) batteries [36,37]. They are widely used in portable electronics like smartphones, laptops, and electric vehicles, offering cost-effective and eco-friendly alternatives to disposable batteries while reducing long-term waste [38,39].

2.2.1. Lead-acid

A lead-acid battery consists of lead dioxide (PbO_2) anode and a cathode composed of sponge-like lead (Pb), while its electrolyte is made of cost-effective, non-flammable sulfuric acid [36]. During the discharge of lead acid batteries, the lead ions (Pb^{2+}) within the battery engage in a chemical reaction with the electrolyte, leading to the formation of lead sulfate ($PbSO_4$) crystals. During the charging process, these crystals undergo a transformation, reverting to their elemental states as Pb and PbO_2 [36].

The lead-acid battery has benefits including a long cycle life of up to 1500-5000 cycles [32]. These batteries are also known for their recyclability and cost-effectiveness which holds the largest market share among rechargeable batteries in the automotive industry, primarily due to the abundance of raw materials [36,40,41]. Nevertheless, one the major concerns about these batteries is toxicity [42]. Moreover, these batteries tend to be relatively heavy and have an energy density within the range of 30 to 50 Wh/kg which is not high compared to the other rechargeable batteries [43]. The open circuit voltage of lead-acid batteries remains stable at 2.1 volts [36]. It is also worth mentioning that they lack fast-charging capabilities and do not offer a high depth of discharge [36]. Additionally, the coulombic efficiency of these batteries are 90-95% [44].

2.2.2. NiCd

NiCd batteries consist of a metallic Cd anode, a nickel hydroxide ($Ni(OH)_2$) cathode, and an aqueous potassium hydroxide (KOH) electrolyte [45,46]. During the discharge OH^{+2} and $Ni(OH)_2$ on the cathode side and $Cd(OH)_2$ on the anode side are produced. This reaction reverses during the charging process [47].

NiCd batteries have several advantages. Notably, the NiCd battery offers an energy density ranging from 50 to 75 Wh/kg [40], and a long cycle life that spans from 3,500 to 50,000 cycles [48],

 doi:10.20944/preprints202402.0784.v1

with the coulombic efficiency of 70-80% [44]. It has resilience under mechanical and electrical stress [40], does not release gas [46], has a high depth of discharge, and is suitable for a wide range of industrial applications, including remote controls, aircraft, and diesel engine starters[49]. The main drawbacks of these batteries are the cost [40], and the toxic and heavy materials [50]. Additionally, NiCd batteries suffer from a relatively high self-discharge rate. The open circuit voltage of the nickel-cadmium battery is 1.2 Volts [51].

2.2.3. Ni-MH

Ni-MH batteries are made of a nickel hydroxide anode, a metal hydride cathode, and an electrolyte based on aqueous potassium hydroxide [52]. Hydroxide ions are generated at the negative electrode through the decomposition of water within the electrolyte, while the positive electrode experiences oxidation of the nickel hydroxide [53].

The Ni-MH battery has a high energy density of more than 70 Wh/kg, a power density of more than 200 W/kg, and a broad operational temperature range [54]. It is often considered a safe and environmentally friendly option [55]. Furthermore, its lifespan is high, typically reaching up to 3000 cycles [56], and the coulombic efficiency is 70-80% [44]. The Ni-MH battery has a notable self-discharge rate, and a limited DOD [57,58]. The open circuit voltage of the Ni-MH battery is between 1.25 and 1.35 V [59].

2.2.4. Li-ion

Lithium-ion batteries typically consist of a graphitic carbon anode with a layer structure. The cathode in these batteries are made of a lithiated metal oxide compounds, including lithium cobaltite (LCO), mixed oxides of nickel, cobalt, and aluminum (NCA), nickel, cobalt, and manganese (NCM), lithium manganese dioxide spinel (LMO), and lithium iron phosphate (LFP) [60]. The electrolyte is also a solution of lithium salts dissolved in organic carbonates [60]. During the charging process, lithium atoms within the cathode transform into lithium ions and migrate towards the carbon-based anode, depositing on the anode surface as lithium atoms [50]. Additionally, these batteries perform with a high coulombic efficiency of more than 95% [44].

The lithium-ion battery have benefits including a long cycle life of up to 3000 cycles, high energy density ranging from 75 to 125 Wh/kg [61], and minimal self-discharge [62]. Lithium-ion batteries are, however, sensitive to overvoltage [45]. Their open circuit voltage typically falls within the range of 3 to 4.2 volts [63].

2.3. Basic geometries

The geometry of battery electrodes plays a key role in determining both battery application and performance [30,64]. The two fundamental figures of merit for batteries are energy density and power density. Increasing the energy density, however, can negatively impact power density. This occurs due to the longer transport distance for ions within the battery structure, ultimately impeding the rate of energy delivery [65]. Consequently, the manipulation of battery geometry can create a balance between power density and energy density. Battery geometries are shaped by their component architecture, including designs such as thin film [66], 3D porous structure [67], and fiber designs [68]. As these component architectures come together, they result in various battery cell configurations such as sandwich, in-plane, concentric tube, and fiber arrangements. Among these, thin film structures and porous frameworks (grid) stand out as the most common and important forms [30].

2.3.1. Thin film

The thin film structure is one the most widely recognized configuration which is readily available in the market and can be fabricated through conventional methods [69]. It is made of rectangular electrodes stacked on top of each other which can improve the performance through surface area [70]. This structure offers a notable advantage through reduced resistance and a shorter Li+ diffusion length, contributing to an increase in power density [71]. In contrast, the energy density

 doi:10.20944/preprints202402.0784.v1

within this configuration is comparatively lower than in other structures. This arises from the limited active content that can be accommodated in a thin film and further modifications are required to enhance the overall energy density [72].

2.3.2. 3D Porous structure

The porous structure represents an innovative geometry that can be effectively fabricated using techniques such as 3D printing, in contrast to traditional methods, which often struggle to control intricate geometric structures. Creating pores in various scales in the structure and increasing electrode thickness facilitate the ion transport within the structure which is beneficial to make a balance between energy and power density. An additional advantage of this design lies in its capacity for electrolyte penetration, enhancing the involvement of ions in electrochemical reactions and improving the battery performance [73–82].

2.4. Impact of 3D Printing on Battery Performance

The advantages that 3D printing provides for the battery fabrication includes the ability to achieve high-resolution designs [83], ensuring mechanical stability [84], optimizing energy density and power density [84], customizing battery structures for specific applications [85], accommodating a wide range of battery sizes [86], having the fabrication processes with fewer steps and shorter production times [84], enabling rapid fabrication [87], and the ability to create all-solid-state batteries [88]. Moreover, 3D printing in the context of batteries minimizes material wastage which is beneficial for environmental sustainability [89].

- High Resolution and Mechanical Stability: The advent of 3D printing technology have revolutionized the precision and resolution of the battery designs which directly affects the energy and power density and the overall battery performance [90–97]. Furthermore, the ability to fabricate high-resolution geometries through 3D printing results in enhanced mechanical stability [94]. Engineering designs at the microscopic scale make it possible to control the battery structure precisely, ensuring enhanced mechanical performance. Battery properties, particularly during electrochemical reactions when components undergo changes that can impact structural integrity, benefit from mechanical stability [98]. With 3D printing advantages in high resolution, the risk of electrode breakage and battery failure due to structural instability is eliminated which increases the overall reliability of the battery [99].
- Energy density and power density: 3D printing with the ability to control the design makes it possible to increase the active material loading inside the structure in the less volume which results in higher energy density [100–103]. On the other hand, 3D printing ability to finely control the geometry of battery components plays a critical role in elevating this energy transfer rate within the structure, ultimately resulting in higher power density [104–106].
- Customizability and size: One of the advantages of 3D printing is the design control which leads to the customizability of the structure. Furthermore, depending on the method and the device resolution, the size can be controlled, and the part can be fabricated in a wide range of scales for the production of miniaturized batteries [107,108].
- Efficient Production Process: In contrast to the conventional method, which consist of multiple steps including slurry preparation, tape casting, material drying, calendaring, material cutting, assembly, electrolyte filling, and final packaging, 3D printing offers notable efficiency. In the 3D printing process, the steps include material preparation, part geometry design, 3D printing, assembly, and optional electrolyte filling, depending on the chosen 3D printing method [109–112]. One of the advantages of 3D printing in battery production is the potential reduction in

 doi:10.20944/preprints202402.0784.v1

fabrication time which is attributed to the straightforward process with fewer steps. Nevertheless, it is crucial to note that the overall fabrication time depends on the specific method employed and any post-treatment requirements [31].

- Minimized Material Wastage and Environmental Sustainability: The computer-driven design and fabrication of batteries using 3D printing minimizes material wastage [113], thus lowering production costs [114] and promoting environmental sustainability [30].
- Ability to fabricate all-solid-state batteries: Solid-state batteries, utilizing solid electrolytes instead of liquid counterparts, offer high dimensional integrity, excellent mechanical properties, and enhanced safety [115]. 3D printing, with its precision and design control, facilitates the engineering and fabrication of solid-state electrolytes compatible with electrode configurations which results in the all-solid-state batteries through which all the components can be printed on top of each other. This approach eliminates the need for glove boxes, making production more cost-efficient and environmentally friendly [116–119].

2.5. Goals of geometric design for batteries

Specific designs in batteries can solve many scientific or engineering issues and provide the battery with the opportunity to improve the overall performance in specific applications. The main purpose of controlling the design in batteries is improving the most important properties including energy density, power density, cycle life, and safety.

- Energy density and power density: The design helps the user to fabricate the battery component based on the mechanical configuration of the device which makes it possible to customize the shape and size of the battery. With the design freedom, batteries can be fabricated with complicated integration and controlled distance between the components to receive the best properties of the battery. The 3D printed electrodes facilitate the ion transfer which results in high energy density and high power density [30,120,121].
- Cycle life and safety: The arrangement of electrodes and the distribution of active materials impact uniform charge and discharge cycles, thus affecting cycle life [122]. Additionally, the geometry can improve thermal management, preventing overheating and enhance safety [123]. Moreover, proper separator and electrolyte design, as well as internal pressure management mechanisms, contribute to safety and longevity [102,124].

3. Review

In recent years, 3D printing technology has emerged as a groundbreaking approach for the fabrication of batteries, offering advantages in terms of design flexibility, customization, and rapid prototyping. Various 3D printing methods with their unique characteristics and potential applications have been explored for battery manufacturing. This literature review aims to introduce four of the most promising 3D printing methods for battery fabrication: direct ink writing (DIW), fused filament fabrication (FFF), inkjet printing (IJP), and stereolithography (SLA) (Figure 2). First the principles, advantages, limitations, will be examined and then recent advancements associated with these techniques will be discussed revealing their contributions to the field of energy storage.

 doi:10.20944/preprints202402.0784.v1

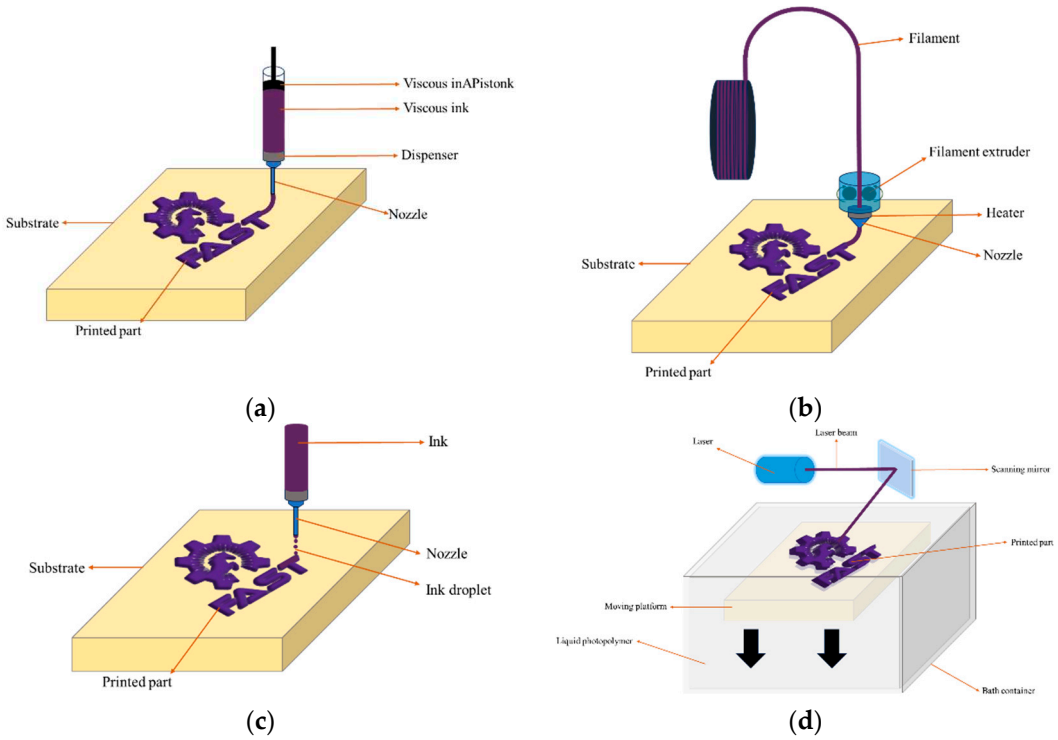

Figure 2. Illustration of (a) DIW; (b) FFF; (c) IJP; and (d) SLA.

3.1. DIW

DIW is a 3D printing technique employed in battery fabrication, relying on the precise extrusion of inks or pastes through a nozzle to create an integrated three-dimensional structure. In DIW for battery manufacturing, the ink typically comprises active materials, conductive materials, binders, and solvents. The extrusion process is characterized by high controllability governed by parameters such as pressure, speed, and nozzle size, allowing for the precise positioning of materials [125–127].

One of its features is the resolution it offers over the creation of complex structures and well-aligned lattice designs which are advantageous for achieving high porosity and facilitating ion transport in energy storage devices with the least material wastage. The resolution of 3D structures printed using DIW is determined by factors such as nozzle diameter, applied pressure, and ink characteristics, typically ranging from 1 to 250 micrometers [125,127–129]. Furthermore, compared to other 3D printing methods, DIW can be a more affordable choice, making it accessible to a broader range of applications. Moreover, this method is known for its ease of fabrication and typically requires minimal or no post-production treatment [130]. Another key advantage of DIW is the flexibility in material selection, allowing for the use of a wide range of printing feedstocks including metals, ceramics, polymers, and composites which empowers the users to select materials that align with the specific applications [127,131]. Moreover, this method has the advantage of printing multi-material structures through the use of multi-nozzle printers or by employing a print-pause-print strategy and swapping syringes containing different materials [132–136].

One of the challenges of DIW is the need for specific techniques to prepare desirable ink formulations. The ink must exhibit viscoelastic and shear-thinning properties to resist gravity-induced deformation and capillary forces during the printing process. The selection of materials and their rheological properties directly influences the quality of the final printed components, contributing to the time-consuming nature of the method [137]. Another limitation lies in the mechanical properties of DIW-fabricated structures. While DIW has precision and customization, the resulting printed components may exhibit poor mechanical properties compared to conventionally manufactured batteries [138].

Some examples of DIW of batteries include:

 doi:10.20944/preprints202402.0784.v1

Li et al. used the advantages of DIW to develop a highly conductive reduced graphene oxide (rGO)/Super-P aerogel composite anode with high resolution and complex hierarchically porous structure. The optimized rGO/Super-P aerogel electrode demonstrated a superior initial discharge capacity of 848.4 mA h at 80 mA cm^{-2}, a 14.9% improvement over traditional graphite electrodes with 61.8% capacity retention over 100 cycles. Additionally, the coulombic efficiency was measured higher than 95% over 100 cycles [139].

In another study, Zhu et al. fabricated high resolution metallic 3D-Zn electrode structures using DIW. These designs with submillimeter sizes exhibited low electrical resistivity and high mechanical stability. The results showed that the cell operated over 50 cycles at high discharge rates of 25 mA cm^{-2} achieving an average specific capacity of 214.85 mAh g^{-1} which was the highest achieved amount compared to the similar electrodes fabricated by other methods. Moreover, the capacity retention over 50 cycles was 108% and the average coulombic efficiency of approximately 87% was achieved [140].

Liu et al. developed $Li_{1.3}Al_{0.3}Ti_{1.7}(PO_4)_3$ (LATP) electrolyte for solid-state electrolytes in lithium batteries using DIW with post-heat treatment to enhance ceramic density, completing the formation of the final LATP solid-state electrolyte structures. They shaped these materials into various forms while maintaining high ionic conductivity 4.24×10^{-4} S cm^{-1} which is higher than the ones prepared by other methods (2.05×10^{-4} S cm^{-1}). Through this process, the solid-state battery exhibited a high discharge capacity of 150 mAh g^{-1} at 0.5 C, along with 84% capacity retention with an average coulombic efficiency of approximately 100% over 100 cycles [141].

Tao et al. employed DIW to fabricate high-capacity 3D $LiNi_{0.8}Mn_{0.1}Co_{0.1}O_2$ (NMC) cathodes. This innovative approach increased the contact area, shortened diffusion paths, and reduced stress. The specific discharge capacities for the first and 800th cycles were measured at 178.6 and 107.5 mAh g^{-1}, respectively, showing a capacity retention of 60.2% over the entire 800 cycles with an average coulombic efficiency of approximately 99.9% at a current density of 1 C. These results were superior compared to those achieved through conventional methods, which were equal to 162.3 mAh g^{-1} in the first cycle and 88.3 mAh g^{-1} which show a capacity retention of 54.4% in the 800th cycle [142].

Li et al. used DIW to fabricate a square grid electrode structure for lithium-ion batteries. The ink was prepared by combining $LiFePO_4$ (LFP), MWCNTs, and PVDF powder, forming a homogenized paste with NMP as a solvent. The results demonstrated the initial discharge capacity of 143.2 mA h g^{-1} at 0.5 C, aligning with the theoretical specific capacity of 170 mA h g^{-1}. Moreover, the charge and discharge specific capacities remained stable, sustaining at approximately 150 mA h g^{-1} even after 100 cycles at 0.5 C showing the capacity retention of 105%. Furthermore, the coulombic efficiency was measured around 99.9% over 500 cycles at 5C [143].

Rasul et al. utilized DIW to embed highly aligned boron nitride (BN) nanosheets into PVdF polymer composite electrolytes (CPE) with complex structure. The achieved ionic conductivity was 6.74 x 10^{-4} S cm^{-1}. The initial charge capacity of the cells prepared with CPE-BN was 156 mAh g^{-1}, which was comparable to the theoretical capacity of 165 mAh g^{-1}. The cell exhibited a consistent discharge capacity of 132 mAh g^{-1} over 130 cycles at 1C rate (140 mA g^{-1}) and a capacity retention of 90% after 250 cycles [144].

Liu et al. utilized DIW for fabricating a comb-like structure SiO@C/graphite anode and LFP cathode for lithium-ion batteries. The full cell assembled with both the printed anode and cathode exhibited a specific capacity of 110 mAh g-1 for the initial cycles, decreasing to 75 mAh g-1 at 0.3 C after 40 cycles. Notably, the capacity retention remained at 68.2% after 80 cycles, and the initial coulombic efficiency of 70% improved to 100% after the first few cycles [145].

Table 1 provides a summary and comparison of the electrochemical performance achieved through the direct ink writing method for batteries. As evident from the results in Table 1, this technique is versatile which proves its applicability to enhance battery efficiency in the fabrication of different battery components including anode, cathode, and solid electrolyte.

 doi:10.20944/preprints202402.0784.v1

Table 1. Summary and comparison of electrochemical performance for DIW of batteries.

Printed component	Discharge Capacity	Coulombic efficiency	Cycle numbers	Reference
Anode: rGO/Super-P aerogel	848.4 mA h at 80 mA cm−2	More than 95%	100	[139]
Anode: metallic Zn	214.85 mAh g−1 at 25 mA cm−2	87%	650	[140]
Electrolyte: LATP	150 mAh g-1 at 0.5 C	100%	100	[141]
Cathode: NMC	107.5 mAh g−1 at a current density of 1 C	99.9%	800	[142]
Cathode: LFP	150 mA h g−1 at 0.5 C	99.9%	100 - 500	[143]
Electrolyte: BN-PVDF	132 mAh g−1 at 1C rate	N/A	130	[144]
Anode: SiO@C/graphite Cathode: LFP	75 mAh g-1 at 0.3 C	100%	40	[145]

Figure 3 illustrates the capacity retention of these cells. As can be seen, high-capacity retentions, even exceeding 100%, can be achieved through the fabrication of battery components using this method. This is promising for fabricating high-performance battery cells with a long cycle life.

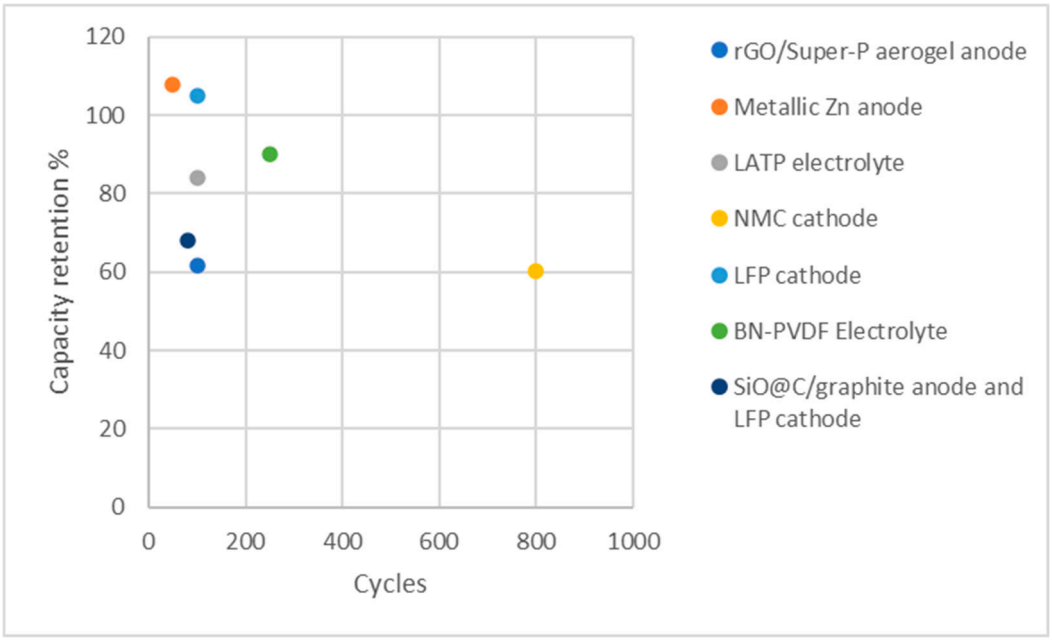

Figure 3. Capacity retention of the cells fabricated by DIW.

3.2. FFF

FFF is a widely adopted 3D printing technique, including in the field of battery manufacturing. It is used widely by various manufacturers and open-source 3D printing communities, representing the broader category of 3D printing technologies utilizing melted filament deposition. On the other hand, fused filament modeling (FDM), trademarked by Stratasys, is a proprietary 3D printing technology using FFF associated only with Stratasys machines [146]. This process operates by melting a thermoplastic filament in a heated nozzle. FFF was radically reduced in price and improved performance due to the open source self-replicating rapid prototype (RepRap) project and is now the

 doi:10.20944/preprints202402.0784.v1

most popular form of 3D printing [147–149]. Within the context of 3D-printed batteries, FFF is employed to produce essential battery components including electrodes, solid state electrolyte, and current collector. For this purpose, FFF offers the capability to integrate conductive materials into the filament, creating conductive pathways within the battery structure [150–153]. FFF is a widely adopted 3D printing technique, including in the field of battery manufacturing. This process operates by melting a thermoplastic filament in a heated nozzle. One of the advantage of FFF 3D printing is that unlike DIW that requires specialized inks, it eliminates the need for ink preparation which simplifies the printing process [108]. Furthermore, its ability to create complex battery designs with the resolution of 50 to 200 μm is a feature that enables the fabrication of battery components that may be challenging to produce using conventional methods [108,154].

FFF generates minimal waste during the printing process which is in alignment with sustainable manufacturing practices [154] and is a mature distributed recycling technology [155–158]. Additionally, the accessibility of FFF along with the user-friendly interface and ease of operation, make it an economical choice for battery production [150,159]. In addition to the low cost, FFF printers are capable of high production rates, suitable for both prototyping and large-scale manufacturing of battery components [160]. Furthermore, FFF is capable of printing multi-material, which enables its ability to print various battery components on top of each other [161,162].

Despite the advantages, FFF of batteries presents its own drawbacks. One of the most important challenges of FFF 3D printing is the material selection to formulate a suitable filament which often leads to difficulties in filament fabrication [30]. The integration of active and conductive particles, necessary to enhance electrochemical performance, can diminish the overall printability of the filament which makes the production process more complex [163]. Moreover, this incorporation can increase the viscosity of the filament which results in the risk of nozzle clogging during the printing operation [150,164]. Beyond these material-related issues, the printed part has weak mechanical properties in the z-direction due to challenges in ensuring proper layer adhesion [31,114,165] and the inherent anisotropy of the process [166]. Furthermore, the printing process can result in components with lower surface quality [31,167].

Some examples of FFF of batteries include:

Beydaghi et al. utilized FFF to create 3D printed Si-based electrodes for Li-ion batteries. They fabricated the PLA filament as the polymeric matrix along with carbon-based conductive additives, and Si nanoparticles. The results showed that the coulombic efficiency progressively increased from 90% in the first cycle to 96% after 10 cycles which remained stable up to 350 cycles. At the 350th cycle, the electrode exhibited a specific capacity of 327 mA h g^{-1}, coupled with capacity retention of 95% at the current density of 20 mA g^{-1} [168].

Maurel et al. developed a 3D printable graphite/PLA filament through optimizing the graphite content of the filament along with the plasticizer for lithium-ion battery electrodes. Among compositions, the one with the highest amount of conductive additives achieved the initial capacity of 93 mAh g^{-1} which reached the highest specific capacity of 200 mAh g^{-1} (215% capacity retention) at the current density of 18.6 mA g^{-1} (C/20) over 6 cycles. These results were comparable with the theoretical capacity of the active materials [154].

In another work, Maurel et al. produced PLA/LFP as positive electrode and PLA/SiO_2 as the separator for Li-ion batteries. The results when PLA/Graphite was used as the negative electrode showed that the composition made of the 10% of the conductive material had the highest specific capacity of 165 mAh g^{-1} at C/20 over 30 cycles (97% capacity retention) close the theoretical capacity [169].

Gao et al. improved Aqueous Rechargeable Zinc-Ion Batteries by designing hierarchical core–shell cathodes by integrating the FDM and atomic layer deposition (ALD). In their work, the FFF printed porous carbon network provided an electron-conductive core and ion diffusion channels, while V_2O_5 deposited through the ALD served as an active shell. This resulted in enhanced battery performance, with a specific capacity of 425 mAh g-1 at 0.3 A g^{-1}, and 233 mAh g^{-1} at 3 A g^{-1} current density. The capacity at 3 A g^{-1} current density reduces to 183 mAh g^{-1} after 200 cycles and 133 mAh

 doi:10.20944/preprints202402.0784.v1

g^{-1} after 800 cycles showing 78.5% and 57.1% capacity retention, respectively. Additionally, the coulombic efficiency was around 99.9% [170].

Foster et al. utilized a graphene/PLA filament with controllable graphene content, ranging from 1 to 40 wt.%, enabling the creation of 3D printed freestanding anodes with sufficient conductivity and printability, eliminating the need for a copper current collector. The results showed that the initial specific capacity was 500 mAh g^{-1} which reaches to about 100 mAh g^{-1} with the coulombic efficiency around 99.9% at 40 mA g^{-1} over 200 cycles. Comparing the achieved capacity with the theoretical capacity of graphite (375 mAh g^{-1}) and graphene (744 mAh g^{-1}), it can be concluded that this capacity lies between these two values. It is clear that the 3D printed anode exhibits graphene-like electrochemical performance [171].

Hu et al. produced TPU-LFP, TPU-LTO, TPU-Graphite, and TPU-NCM filaments and printed high-performance cathodes and anodes via FDM. The cells made with TPU-LFP cathode showed the initial capacity of 114.1 mAh g-1 with 99.12% capacity retention (113.1 mAh g^{-1}) with 99.75% coulombic efficiency after 200 cycles, and 98.9% capacity retention after 400 cycles. Moreover, the cell made by the TPU-LTO anode showed 117.2% capacity retention increasing from 102.4 to 120.0 mAh g-1 with 100.39% coulombic efficiency over 200 cycles, and 97.94% capacity retention with 99.04% coulombic efficiency over 270 cycles. Additionally, the full cell assembled by the TPU-LFP cathode and TPU-LTO anode exhibited 97.1% capacity retention at the rate of 0.3 C and a coulombic efficiency of 97.4% after 50 cycles. All of the results indicate higher capacity retention in this work compared to the similar ones [172].

In another study, Maurel et al. developed a 3D-printable polyethylene oxide/lithium bis(trifluoromethanesulfonyl)imide (PEO/LiTFSI) filament which was designed for use as the electrolyte in lithium-ion batteries. The achieved ionic conductivity was 2.18 x 10^{-3} S cm^{-1} at 90°C which shows the capability of FFF in fabricating solid-state electrolytes [173].

Table 2 provides a summary of examples of FFF printed battery components, including anode, cathode, separator, and electrolyte which shows the potential of this method to fabricate all-solid-state batteries.

Table 2. Summary and comparison of electrochemical performance for FFF of batteries.

Printed component	Discharge Capacity	Coulombic efficiency	Cycle numbers	Reference
Anode: PLA/Si/graphene	327 mA h g^{-1} at the current density of 20 mA g^{-1}	96%	350	[168]
Anode: PLA/Graphite	200 mAh g^{-1} at the current density of 18.6 mA g^{-1} (C/20)	N/A	5	[154]
Cathode: PLA/LFP Separator: PLA/SiO_2	165 mAh g^{-1} at C/20	N/A	~30	[169]
Cathode: Carbon/ V_2O_3	183 mAh g^{-1} at 3 A g^{-1} current density	99.99%	200	[170]
Anode: PLA/Graphene	100 mAh g^{-1} at 40 mA g^{-1}	99.9%	200	[171]
Cathode: TPU-LFP	113.1 mAh g-1 at the rate of 0.3 C	99.75%	200	[172]
Anode: TPU-LTO	120.0 mAh g-1 at the rate of 0.3 C	100.39%	200	[172]

Figure 4 illustrates the capacity retention of the FFF printed cells as a funciton of cycles. As can be seen, the fabricated cells show high-capacity retention.

 doi:10.20944/preprints202402.0784.v1

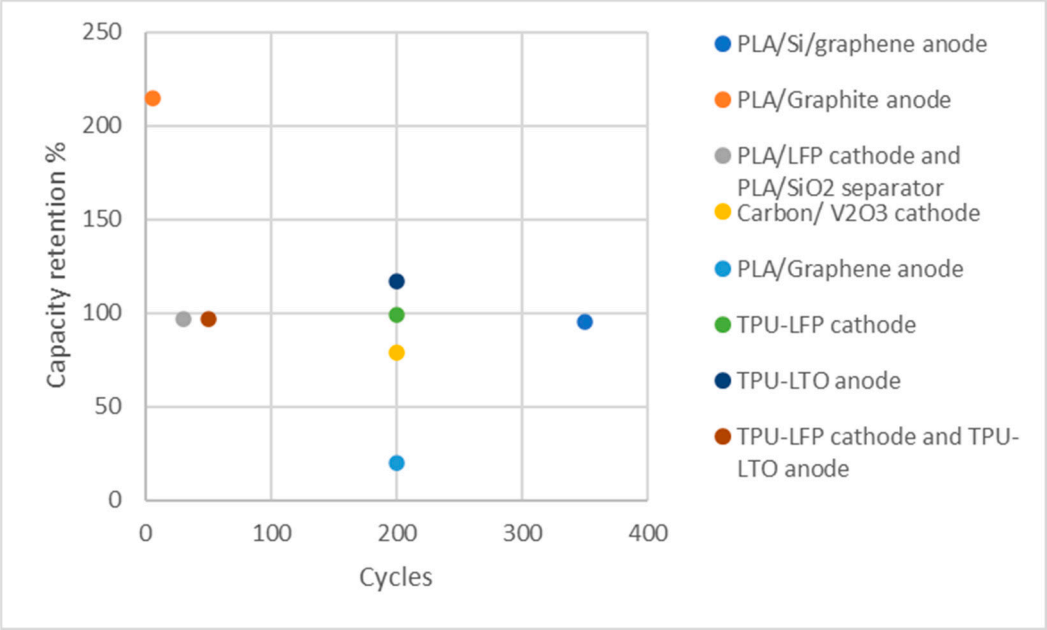

Figure 4. Capacity retention of the cells fabricated by FFF.

3.3. IJP

This method operates by selectively depositing small droplets of specialized inks onto a substrate in a layer-by-layer process. The ink contains essential materials for battery components, such as electrodes, electrolytes, and current collectors, finely dispersed within a liquid carrier. After each layer is printed, it may undergo processes like drying or curing before the printer proceeds to deposit the subsequent layer [31,174].

IJP offers numerous advantages in battery fabrication. By depositing precise amounts of the ink only where needed to eliminate waste, IJP ensures that the materials are utilized efficiently which results in minimizing environmental impact and cost [175,176]. Another advantage is its lower viscosity requirement compared to DIW. This characteristic simplifies the formulation and handling of printable inks which makes the IJP practical and adaptable for a wide range of materials and applications [174]. This method is also capable of multi-material deposition which provides the controlled deposition of active materials of battery components [177]. Moreover, the affordability of IJP equipment along with the ease of use make this technique an accessible choice for the battery manufacturing process [138].

Despite the advantages, a uniform printed structure through IJP can be challenging and to maintain both battery performance and structural integrity, fine features and adhesion layers precisely is required [174]. Furthermore, while IJP requires lower ink viscosity than DIW, the properties of the ink, such as viscosity and density, need to be optimized to meet the standards. This optimization is essential to avoid issues including the ink agglomeration and the nozzle clogging [175].

Some examples of IJP of batteries include: Lawes et al. utilized IJP for efficient and cost-effective fabrication of silicon anodes using Si nanoparticles and PEDOT:PSS as a conductive binder. These anodes achieved remarkable cycling performance. The initial capacity was measured 3800 mAh g^{-1} in the first cycle which reduced to 2700 in the following cycles. Moreover, the achieved capacity was more than 1700 mAh g^{-1} at 0.1 C showing the capacity retention of 63% over 100 cycles. The coulombic efficiency starts from 31% and 75% in the first two cycles and increases to 98.6% for the remaining cycles. The electrical conductivity of PEDOT:PSS and reversible deformation properties formed a continuous conductive network, ensuring rapid electron transfer and accommodating SiNP volume changes during charge and discharge [179].

Chen et al. used IJP to fabricate a dendrite-free Zn anode with Ag nano particles for Zn metal batteries. They inkjet-printed Ag nanoparticles-modified carbon cloth (AgNPs@CC) leading to

 doi:10.20944/preprints202402.0784.v1

reducing nucleation overpotential and promoting uniform Zn nucleation. This resulted in the initial discharge capacity of 255 mAh g^{-1} at 5 A g^{-1} reaching 184 mAh g^{-1} after 1200 cycles with only 0.023% capacity fade rate in each cycle with the coulombic efficiency of about 99.5% within 800 cycles. Nonetheless, as reported in this work, the similar anode fabricated without inkjet-printed Ag nanoparticles exhibited a capacity retention rate of 42.9% after 700 cycles [180].

Kushwaha et al. utilized IJP to deposit graphene inks made from graphene nanosheets in ethanol solvent and ethyl-cellulose stabilizer onto different substrate including Cu foil. The print was followed by annealing to achieve conductivity and porosity. The reversible capacity was about 520 mAh g^{-1} with capacity retention of about 87% after 100 cycles at 2C which is a high current density. Furthermore, the initial coulombic efficiency was 95% reaching to more than 99% over 100 cycles [181].

In their other work, Kushwaha et al. used IJP to deposit a graphene layer onto an Al current collector foil, addressing corrosion issues in cathode current collector. This work significantly suppressed corrosion, achieving about 180 mAh g^{-1} initial capacity at C/5 with ~90% capacity retention after 100 cycles [182].

Viviani et al. investigated the impact of carbon-based additives, such as carbon black and multi-walled carbon nanotubes, on the electrochemical performance of inkjet-printed thin-film LTO electrodes in lithium-ion batteries. Between the carbon-based additives, the carbon nanotube electrode achieved the highest specific capacity, reaching 128 mAh g^{-1} at 0.5 C, and exhibited excellent cycle stability with negligible capacity loss (100% capacity retention) and the average coulombic efficiency of 100% over 100 cycles [183].

Kolchanov et al. utilized inkjet printing to fabricate thin-film Li-ion batteries through the optimization of $Li_{1.2}Mn_{0.54}Ni_{0.13}Co_{0.13}O_2$ (LMR) cathode. The study demonstrated comparable discharge capacities 240 mAh g^{-1} between inkjet and conventional methods at 0.01 C rate with 68.7% capacity retention over 70 cycles [184].

These examples are shown Table 3 representing the effectiveness of IJP to improve the battery performance through the fabrication of different battery components.

Table 3. Summary and comparison of electrochemical performance for IJP of batteries.

Printed component	Discharge Capacity	Coulombic efficiency	Cycle numbers	Reference
Anode: Si/ PEDOT:PSS	1700 mA h g^{-1} at 0.1 C	98.6%	100	[179]
Anode: AgNPs@CC	184 mAh g^{-1} at 5 A g-1	99.5%	1200 & 800	[180]
Anode: graphene onto Cu foil substrate	520 mAh g^{-1} at 2C	99%	100	[181]
Current collector: graphene coated Al	180 mAh g^{-1} at C/5	N/A	100	[182]
Anode: LTO	128 mAh g^{-1} at 0.5 C	100%	100	[183]
Cathode: LMR	240 mAh g^{-1} at 0.01 C	N/A	70	[184]

Figure 5 illustrates the capacity retention of the IJP printed cells. As can be seen, AgNPs@CC anode fabricated by this method shows high capacity retention of 100% over 1200 cycles which is noticeable and indicates the high electrochemical performance of the cell.

Preprints.org (www.preprints.org) | NOT PEER-REVIEWED | Posted: 14 February 2024 doi:10.20944/preprints202402.0784.v1

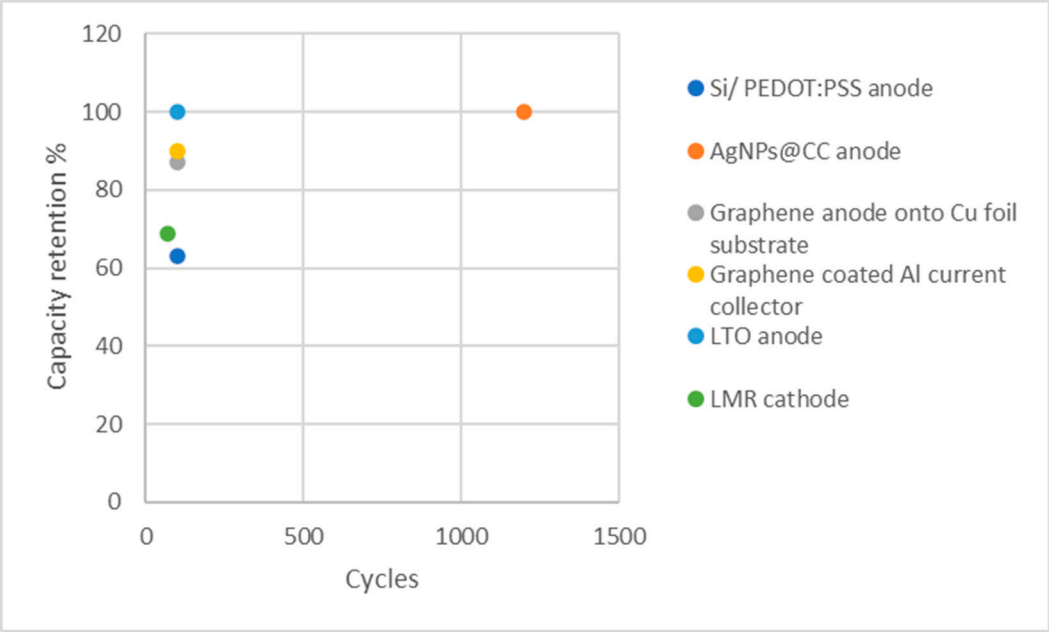

Figure 5. Capacity retention of the cells fabricated by IJP.

3.4. SLA

SLA, a prominent light-assisted 3D printing technology, operates by employing a light source to solidify a polymer resin selectively layer by layer. The versatility and precision offered by SLA make it a valuable tool in various industries, with notable applications emerging within the energy storage systems [31,185,186].

One of the advantages of SLA is its high resolution, which can reach up to 0.5 micrometers which makes it a well-suited for applications demanding complex geometries [30,97,187,188]. Additionally, SLA is nozzle-free, setting it apart from some other 3D printing methods. This feature eliminates the risk of nozzle clogs or filament feed issues which makes the printing process more reliable and uninterrupted [30,96,189]. Furthermore, objects produced through SLA generally exhibit smooth and highly detailed surface finishes [94,190]. The technique also excels in layer bonding due to its chemical curing process, resulting in strong layer-to-layer adhesion. This attributes to high mechanical strength, structural integrity, and durability of printed objects [191].

The preparation of printable resins containing the right blend of active materials, photoinitiators, and monomers can be a complex process [30]. Flowability of the resin is another crucial consideration. If the flowability is not properly balanced, it can hinder the printing process and result in suboptimal print quality [30]. Additionally, the refractive index of the resin is of great importance. An unsuitable refractive index can cause UV light to scatter within the resin, which can result in defects, incomplete curing, compromised mechanical properties, and a lack of printing accuracy [30,185,192]. An unsuitable refractive index can cause UV light to scatter within the resin, which can result in defects, incomplete curing, compromised mechanical properties, and a lack of printing accuracy [30,185,192]. SLA 3D printing system tends to be relatively expensive high cost for industrial applications too [96]. The price per printed object, especially for simpler designs or smaller projects, might be comparable to those from other 3D printing methods. The overall affordability of SLA technology may vary depending on factors such as the complexity of the printed objects and the specific requirements of the application. Furthermore, post-processing requirements are often necessary for SLA prints. These post-processing steps, such as excess resin cleaning, can be time-consuming and may influence the final accuracy and surface finish of printed objects [31].

Some examples of SLA of batteries include: He et al. developed a solid polymer electrolyte containing lithium bis(trifluoromethanesulfonyl)imide (LiTFSI) for all-solid-state lithium metal batteries using SLA. The printed structure showed high ionic conductivity of 3.7×10^{-4} S cm^{-1} with

 doi:10.20944/preprints202402.0784.v1

initial specific capacity of 166 mAh g^{-1} at 0.1 C with 78% capacity retention and the coulombic efficiency around 100% over 250 cycles [116].

Chen et al. utilized SLA to fabricate Poly (ethylene glycol) (PEG)-base gel polymer electrolyte containing $LiClO_4$ salt. The cell was made by a 3D printed solid electrolyte flown by LTO and LFP as electrodes. The results indicated that the electrolyte can deliver high ionic conductivity of 4.8×10^{-3} S cm^{-1} with delivered the discharge capacity of 1.4 µAh cm^{-2} over 2 cycles at 5 µA current which showed the potential of this method in the fabrication of the gel-based electrolyte for lithium ion batteries [193].

Norjely et al. employed SLA to fabricate a polyurethane acrylate (PUA)-based gel polymer electrolyte containing lithium perchlorate ($LiClO_4$) for solid-state lithium-ion batteries. They concluded that the ionic conductivity of the printed solid electrolyte was high equal to 1.24×10^{-3} S cm^{-1} showing the method promising in the fabrication of the solid-state lithium ion batteries [194].

Zekoll et al. used SLA to create 3D templates from structured ceramic-polymer solid electrolytes made by $Li_{1.4}Al_{0.4}Ge_{1.6}(PO_4)_3$ (LAGP). These electrolytes were composed of a 3D ceramic scaffold with the channels filled by non-conducting polymers including polypropylene or epoxy polymer leading to a high ionic conductivity of 1.6×10^{-4} S cm^{-1} along with the high mechanical stability [117].

Lee et al. employed DLP printing for making high conductivity poly(ethylene oxide) (PEO) solid polymer electrolyte. These printed electrolytes exhibited an ionic conductivity of 3×10^{-4} S cm^{-1} [195].

Katsuyama et al. utilized SLA 3D printing and pyrolysis to fabricate hard carbon microlattices as a free-standing anode for sodium ion batteries. The highest specific capacity was 225 mAh g-1 at 5 mA g−1 with the coulombic efficiency of 80% in the initial cycle reaching to 99.4% over the 2nd cycle. The capacity retention was measured about 80% over 100 cycles [196].

Ye et al. employed a DLP printer to create a Si/PEDOT:PSS/PEG (20/5/60) electrode with commercial silicon nanoparticles for lithium-ion batteries. Their aim was to maximize energy storage while minimizing battery weight. In their work, PEDOT:PSS served as the conductive component. The results demonstrated the structural integrity and flexibility of the printed part. Battery performance indicated that this method holds promise for fabricating silicon-based anodes, with an improved coulombic efficiency of up to 86.3% after 125 cycles. The initial discharge capacity of 1539 mAh g^{-1} and a reversible capacity of 1105 mAh g^{-1} (72% capacity retention) at 800 mA g−1 current density [197].

Table 4 shows that until now, much of the research conducted on SLA printing of batteries focused on gel-based/solid electrolyte.

Table 4. Summary and comparison of electrochemical performance for SLA of batteries.

Printed component	Discharge Capacity	Coulombic efficiency	Cycle numbers	Other properties	Reference
Electrolyte: LiTFSI	166 mAh g–1 at 0.1 C	100%	250	Ionic conductivity: 3.7 × 10–4 S cm–1	[116] [116]
Electrolyte: PEG-base gel polymer	1.4 µAh cm-2 at 5 µA	N/A	2	Ionic conductivity: 4.8 × 10–3 S cm–1	[193] [193]
Electrolyte: PUA-base gel polymer	N/A	N/A	N/A	Ionic conductivity: 1.24 × 10–3 S cm–1	[194] [194]
Electrolyte: LAGP solid electrolyte	N/A	N/A	N/A	Ionic conductivity: 1.6 × 10–4 S cm–1	[117] [117]
Electrolyte: PEO solid electrolyte	N/A	N/A	N/A	Ionic conductivity: 3 × 10–4 S cm–1	[195] [195]

 doi:10.20944/preprints202402.0784.v1

Anode: hard carbon microlattices	225 mAh g-1 at 5 mA g−1	99.4%	2	N/A	[196] [196]
Anode: Si/PEDOT:PSS/PEG	1105 mAh g-1 at 800 mA g−1	86.3%	125	N/A	[197] [197]

Figure 6 illustrates the capacity retention of the cells assembled by the SLA printed battery component.

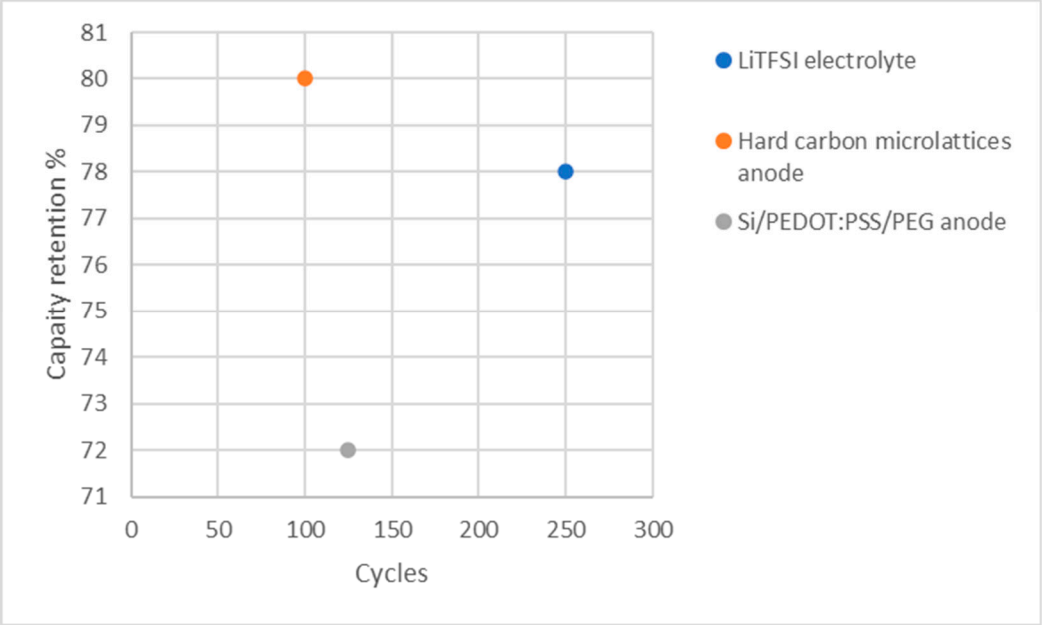

Figure 6. Capacity retention of the cells fabricated by SLA.

4. Discussion

It is clear from this review of experimental results that closely align with theoretical electrochemical performance that 3D printing methods for battery fabrication are promising. There is potential for 3D printing to be incorporated in manufacturing high-performance batteries, primarily due to its inherent design freedom. One of the other interesting aspects of 3D-printing batteries is the capability to fabricate solid-state electrolytes which opens the path to developing all-solid-state batteries. This innovation not only could enhance battery performance, but also enables the creation of fully 3D-printed batteries. Compared to batteries with liquid electrolytes, solid-state batteries often exhibit superior performance, particularly in the areas of safety.

It is also clear from this review that a range of 3D printing methods can be used for various battery components. In this regard, DIW and IJP enable the loading of active and conductive materials into printable ink to facilitate the production of desired components. On the other hand, FFF offers a customizable approach by loading these materials into filaments. Additionally, compared to the other methods, it can be seen that for SLA substantial research has been focused primarily on the fabrication of solid electrolytes. Nevertheless, successful fabrication of other battery components, including free-standing anodes [196], demonstrates SLA's potential in broadening battery component fabrication.

3D printing has proven its ability to fabricate battery components using high-performance materials. Silicon, for example, as a major byproduct of the solar photovoltaic (PV) industry [198], stands out as a promising anode material due to its high theoretical capacity (around 3,579 mAh g^{-1}) [199]. The primary challenge associated with utilizing silicon as an anode is the substantial volume change experienced by the material during battery cycling, thereby constraining its application. Various 3D printing methods, including DIW [145], FFF [168], IJP [179], and SLA [197], have successfully produced silicon anodes with high electrochemical performance by addressing the

 doi:10.20944/preprints202402.0784.v1

volume change issue through special structures achievable via 3D printing, as well as by adding carbon additives that can accommodate the volume change of silicon by covering it. Finally, the high resolution and high fabrication rate of SLA as well as the capability to fabricate solid electrolytes and silicon anodes makes it an exceptionally promising candidate for the production of all-solid-state batteries with superior electrochemical performance, as well as high safety, efficiency, and sustainability. Therefore, among various 3D printing methods, the SLA method is particularly promising for battery fabrication. Challenges, however, remain related to the non-conductive and non-active polymer resin and cost considerations. In this regard, the adoption of the free and open-source hardware (FOSH) development of scientific tools approach is promising as it has been shown to decrease capital costs on average by about 90% [200]. Specific technologies for battery research can be extremely cost effective. For example, a USD $20,000 potentiostat and galvanostat used for characterizing thin-film batteries can be replaced with a USD$100 open-source tool [201]. In addition, open battery management is also available [202] including for in situ monitoring of Li-ion cells [203]. There has also been more application specific FOSH such as a maintenance tool for light-EV batteries [204]. Finally, there has been work to make completely FOSH all-iron batteries [205,206], which provides a model for the FOSH 3D printable batteries discussed here. Integrating an open-source toolchain, spanning from material preparation to battery packaging, emerges as a promising approach to reduce fabrication costs and enhance accessibility to 3D printing technologies for battery research and production.

5. Conclusions

The advent of 3D printing marks a potential transformative shift in the fabrication of energy storage devices as it introduces a new potential for rapid innovation and customization for batteries for specific applications. In contrast to traditional manufacturing, the precision of 3D printing coupled to geometrical freedom can be used to improve battery performance and offer more efficient energy storage solutions. Notably, as shown in this review 3D-printing of batteries offer a path to higher energy density, capacity, and overall performance compared to the conventional manufacturing techniques. Overall, the evidence presented through numerous case studies from labs making substantial progress all over the world shows the potential of 3D printing as a promising solution to enhance energy storage capabilities. Furthermore, the design freedom of 3D printing makes the fabrication of complex geometries and structures possible and emerges as another key aspect to improve the energy storage capacities and applications in the future. In addition, 3D printing is a promising method to enable the use of new materials for battery fabrication to improve battery performance. From an environmental protection viewpoint, the waste reduction associated with 3D printing of batteries is a way toward a more environmentally friendly future directly. Indirectly, the improved performance and flexibility in applications as well as the potential to reduce energy storage costs, could have a substantial positive impact in enabling intermittent renewable energy sources to displace fossil fuels. As 3D printing technologies become more accessible, the prospect of cost-effective production for customized batteries is extremely promising.

Author Contributions: Conceptualization, M.M. and J.M.P.; methodology, M.M. and J.M.P. formal analysis, M.M. and J.M.P.; investigation, M.M. and J.M.P.; resources, M.M. and J.M.P.; data curation, M.M. and J.M.P.; writing—original draft preparation, M.M. and J.M.P.; writing—review and editing, M.M. and J.M.P.; visualization, M.M. ; supervision, J.M.P.; project administration, J.M.P.; funding acquisition, J.M.P. All authors have written, read and agreed to the published version of the manuscript.

Funding: This study was supported by the Thompson Endowments and the Natural Sciences and Engineering Research Council of Canada.

Data Availability Statement: Data is available upon request.

Conflicts of Interest: The authors declare no conflicts of interest.

References

1. Electricity in the U.S. - U.S. Energy Information Administration (EIA) Available online: https://www.eia.gov/energyexplained/electricity/electricity-in-the-us.php (accessed on 19 January 2024).
2. Pearce, J.M.; Parncutt, R. Quantifying Global Greenhouse Gas Emissions in Human Deaths to Guide Energy Policy. *Energies* **2023**, *16*, 6074. https://doi.org/10.3390/en16166074.
3. D'Amato, G.; Cecchi, L. Effects of Climate Change on Environmental Factors in Respiratory Allergic Diseases. *Clinical & Experimental Allergy* **2008**, *38*, 1264–1274. https://doi.org/10.1111/j.1365-2222.2008.03033.x.
4. Haines, A.; Kovats, R.; Campbell-Lendrum, D.; Corvalan, C. Climate Change and Human Health: Impacts, Vulnerability, and Mitigation. *The Lancet* **2006**, *367*, 2101–2109. https://doi.org/10.1016/S0140-6736(06)68933-2.
5. Denkenberger, D.C.; Pearce, J.M. Feeding Everyone: Solving the Food Crisis in Event of Global Catastrophes That Kill Crops or Obscure the Sun. *Futures* **2015**, *72*, 57–68. https://doi.org/10.1016/j.futures.2014.11.008.
6. Barnes, D.F.; Floor, W.M. RURAL ENERGY IN DEVELOPING COUNTRIES: A Challenge for Economic Development. *Annu. Rev. Energy. Environ.* **1996**, *21*, 497–530. https://doi.org/10.1146/annurev.energy.21.1.497.
7. Stern, N.H.; Treasury, G.B. *The Economics of Climate Change: The Stern Review*; Cambridge University Press, 2007; ISBN 978-0-521-70080-1.
8. Peters, G.P.; Hertwich, E.G. CO ₂ Embodied in International Trade with Implications for Global Climate Policy. *Environ. Sci. Technol.* **2008**, *42*, 1401–1407. https://doi.org/10.1021/es072023k.
9. Heidari, N.; Pearce, J.M. A Review of Greenhouse Gas Emission Liabilities as the Value of Renewable Energy for Mitigating Lawsuits for Climate Change Related Damages. *Renewable and Sustainable Energy Reviews* **2016**, *55*, 899–908. https://doi.org/10.1016/j.rser.2015.11.025.
10. Pryor, S.C.; Barthelmie, R.J. Climate Change Impacts on Wind Energy: A Review. *Renewable and Sustainable Energy Reviews* **2010**, *14*, 430–437. https://doi.org/10.1016/j.rser.2009.07.028.
11. Global Wind and Solar Energy Share in Electricity Mix 2022 Available online: https://www.statista.com/statistics/1302047/global-wind-and-solar-energy-share-electricity-mix/ (accessed on 26 September 2023).
12. Hub, I.S.K. Wind and Solar Will Provide 50% of Electricity in 2050, BNEF Report Finds | News | SDG Knowledge Hub | IISD.
13. Yu, H.; Helland, H.; Yu, X.; Gundersen, T.; Sin, G. Optimal Design and Operation of an Organic Rankine Cycle (ORC) System Driven by Solar Energy with Sensible Thermal Energy Storage. *Energy Conversion and Management* **2021**, *244*, 114494. https://doi.org/10.1016/j.enconman.2021.114494.
14. Ali, U. Bloomberg New Energy Outlook 2019: The Future of the Energy Sector. *Power Technology* 2019.
15. Adeh, E.H.; Good, S.P.; Calaf, M.; Higgins, C.W. Solar PV Power Potential Is Greatest Over Croplands. *Sci Rep* **2019**, *9*, 11442. https://doi.org/10.1038/s41598-019-47803-3.
16. Garg, P.; Orosz, M.S.; Kumar, P. Thermo-Economic Evaluation of ORCs for Various Working Fluids. *Applied Thermal Engineering* **2016**, *109*, 841–853. https://doi.org/10.1016/j.applthermaleng.2016.06.083.
17. Zhu, Z.; Jiang, T.; Ali, M.; Meng, Y.; Jin, Y.; Cui, Y.; Chen, W. Rechargeable Batteries for Grid Scale Energy Storage. *Chem. Rev.* **2022**, *122*, 16610–16751. https://doi.org/10.1021/acs.chemrev.2c00289.
18. Kebede, A.A.; Kalogiannis, T.; Van Mierlo, J.; Berecibar, M. A Comprehensive Review of Stationary Energy Storage Devices for Large Scale Renewable Energy Sources Grid Integration. *Renewable and Sustainable Energy Reviews* **2022**, *159*, 112213. https://doi.org/10.1016/j.rser.2022.112213.
19. Harper, G.; Sommerville, R.; Kendrick, E.; Driscoll, L.; Slater, P.; Stolkin, R.; Walton, A.; Christensen, P.; Heidrich, O.; Lambert, S.; et al. Recycling Lithium-Ion Batteries from Electric Vehicles. *Nature* **2019**, *575*, 75–86. https://doi.org/10.1038/s41586-019-1682-5.
20. Nair, N.-K.C.; Garimella, N. Battery Energy Storage Systems: Assessment for Small-Scale Renewable Energy Integration. *Energy and Buildings* **2010**, *42*, 2124–2130. https://doi.org/10.1016/j.enbuild.2010.07.002.
21. Joseph, P.K.; Devaraj, E. Design of Hybrid Forward Boost Converter for Renewable Energy Powered Electric Vehicle Charging Applications. *IET Power Electronics* **2019**, *12*, 2015–2021. https://doi.org/10.1049/iet-pel.2019.0151.
22. Ransome, T. Lithium Ion Battery Available online: https://www.renewables4u.com.au/lithium-ion-battery/ (accessed on 19 January 2024).

23. Mottaghi, M.; Rahman, M.; Kulkarni, A.; Pearce, J.M. AC/off-Grid Photovoltaic Powered Open-Source Ball Mill. *HardwareX* **2023**, *14*, e00423. https://doi.org/10.1016/j.ohx.2023.e00423.
24. Mottaghi, M.; Bai, Y.; Kulkarni, A.; Pearce, J.M. Open Source Scientific Bottle Roller. *HardwareX* **2023**, *15*, e00445. https://doi.org/10.1016/j.ohx.2023.e00445.
25. Dhankani, K.C.; Pearce, J.M. Open Source Laboratory Sample Rotator Mixer and Shaker. *HardwareX* **2017**, *1*, 1–12. https://doi.org/10.1016/j.ohx.2016.07.001.
26. Vadivel, D.; Branciforti, D.S.; Kerroumi, O.; Dondi, M.; Dondi, D. Mostly 3D Printed Chemical Synthesis Robot. *HardwareX* **2022**, *11*, e00310. https://doi.org/10.1016/j.ohx.2022.e00310.
27. Wittbrodt, B.T.; Glover, A.G.; Laureto, J.; Anzalone, G.C.; Oppliger, D.; Irwin, J.L.; Pearce, J.M. Life-Cycle Economic Analysis of Distributed Manufacturing with Open-Source 3-D Printers. *Mechatronics* **2013**, *23*, 713–726. https://doi.org/10.1016/j.mechatronics.2013.06.002.
28. Pearce, J.M. *Open-Source Lab: How to Build Your Own Hardware and Reduce Research Costs*; Elsevier, 2013; ISBN 978-0-12-410486-0.
29. Laplume, A.O.; Petersen, B.; Pearce, J.M. Global Value Chains from a 3D Printing Perspective. *J Int Bus Stud* **2016**, *47*, 595–609. https://doi.org/10.1057/jibs.2015.47.
30. Lyu, Z.; Lim, G.J.H.; Koh, J.J.; Li, Y.; Ma, Y.; Ding, J.; Wang, J.; Hu, Z.; Wang, J.; Chen, W.; et al. Design and Manufacture of 3D-Printed Batteries. *Joule* **2021**, *5*, 89–114. https://doi.org/10.1016/j.joule.2020.11.010.
31. Pang, Y.; Cao, Y.; Chu, Y.; Liu, M.; Snyder, K.; MacKenzie, D.; Cao, C. Additive Manufacturing of Batteries. *Adv. Funct. Mater.* **2020**, *30*, 1906244. https://doi.org/10.1002/adfm.201906244.
32. *Battery Technology Handbook*;
33. HISTORY | Primary Batteries. **2009**, 555–564. https://doi.org/10.1016/B978-044452745-5.00003-4.
34. PRIMARY BATTERIES | Overview. **2009**, 22–27. https://doi.org/10.1016/B978-044452745-5.00096-4.
35. When to Use Rechargeable Batteries Available online: https://www.consumerreports.org/electronics-computers/batteries/when-to-use-rechargeable-batteries-a1076298884/ (accessed on 14 January 2024).
36. Lopes, P.P.; Stamenkovic, V.R. Past, Present, and Future of Lead–Acid Batteries. *Science* **2020**, *369*, 923–924. https://doi.org/10.1126/science.abd3352.
37. The Role of Energy Storage in Low-Carbon Energy Systems. In *Storing Energy*; Elsevier, 2016; pp. 3–22.
38. Viswanathan, B. Chapter 12 - Batteries. In *Energy Sources*; Viswanathan, B., Ed.; Elsevier: Amsterdam, 2017; pp. 263–313 ISBN 978-0-444-56353-8.
39. Burheim, O.S. Secondary Batteries. In *Engineering Energy Storage*; Elsevier, 2017; pp. 111–145 ISBN 978-0-12-814100-7.
40. May, G.J.; Davidson, A.; Monahov, B. Lead Batteries for Utility Energy Storage: A Review. *Journal of Energy Storage* **2018**, *15*, 145–157. https://doi.org/10.1016/j.est.2017.11.008.
41. A General Discussion of Li Ion Battery Safety. *Electrochemical Society Interface* **2012**. https://doi.org/10.1149/2.F03122if.
42. Flora, G.; Gupta, D.; Tiwari, A. Toxicity of Lead: A Review with Recent Updates. *Interdisciplinary Toxicology* **2012**, *5*, 47–58. https://doi.org/10.2478/v10102-012-0009-2.
43. Posada, J.O.G.; Rennie, A.J.R.; Villar, S.P.; Martins, V.L.; Marinaccio, J.; Barnes, A.; Glover, C.F.; Worsley, D.A.; Hall, P.J. Aqueous Batteries as Grid Scale Energy Storage Solutions. *Renewable and Sustainable Energy Reviews* **2017**, *68*, 1174–1182. https://doi.org/10.1016/j.rser.2016.02.024.
44. Quansah, D.A. Comparative Study of Electricity Storage Batteries for Solar Photovoltaic Home Systems. Doctoral dissertation, 2008.
45. Marin-Garcia, G.; Vazquez-Guzman, G.; Sosa, J.M.; Lopez, A.R.; Martinez-Rodriguez, P.R.; Langarica, D. Battery Types and Electrical Models: A Review. In Proceedings of the 2020 IEEE International Autumn Meeting on Power, Electronics and Computing (ROPEC); IEEE: Ixtapa, Mexico, November 4 2020; pp. 1–6.
46. Poullikkas, A. A Comparative Overview of Large-Scale Battery Systems for Electricity Storage. *Renewable and Sustainable Energy Reviews* **2013**, *27*, 778–788. https://doi.org/10.1016/j.rser.2013.07.017.
47. Ramachandra Rao, S. Resource Recovery from Process Wastes. In *Waste Management Series*; Elsevier, 2006; Vol. 7, pp. 375–457 ISBN 978-0-08-045131-2.
48. Beaudin, M.; Zareipour, H.; Schellenberg, A.; Rosehart, W. Energy Storage for Mitigating the Variability of Renewable Electricity Sources. In *Energy Storage for Smart Grids*; Elsevier, 2015; pp. 1–33 ISBN 978-0-12-410491-4.

49. Avril, S.; Arnaud, G.; Florentin, A.; Vinard, M. Multi-Objective Optimization of Batteries and Hydrogen Storage Technologies for Remote Photovoltaic Systems. *Energy* **2010**, *35*, 5300–5308. https://doi.org/10.1016/j.energy.2010.07.033.
50. Divya, K.C.; Østergaard, J. Battery Energy Storage Technology for Power Systems—An Overview. *Electric Power Systems Research* **2009**, *79*, 511–520. https://doi.org/10.1016/j.epsr.2008.09.017.
51. Parker, C.D. APPLICATIONS – STATIONARY | Energy Storage Systems: Batteries. In *Encyclopedia of Electrochemical Power Sources*; Elsevier, 2009; pp. 53–64 ISBN 978-0-444-52745-5.
52. Lemaire-Potteau, E.; Perrin, M.; Genies, S. BATTERIES | Charging Methods. In *Encyclopedia of Electrochemical Power Sources*; Elsevier, 2009; pp. 413–423 ISBN 978-0-444-52745-5.
53. Zhu, W.H.; Zhu, Y.; Davis, Z.; Tatarchuk, B.J. Energy Efficiency and Capacity Retention of Ni–MH Batteries for Storage Applications. *Applied Energy* **2013**, *106*, 307–313. https://doi.org/10.1016/j.apenergy.2012.12.025.
54. Abdin, Z.; Khalilpour, K.R. Single and Polystorage Technologies for Renewable-Based Hybrid Energy Systems. In *Polygeneration with Polystorage for Chemical and Energy Hubs*; Elsevier, 2019; pp. 77–131 ISBN 978-0-12-813306-4.
55. Iclodean, C.; Varga, B.; Burnete, N.; Cimerdean, D.; Jurchiş, B. Comparison of Different Battery Types for Electric Vehicles. *IOP Conf. Ser.: Mater. Sci. Eng.* **2017**, *252*, 012058. https://doi.org/10.1088/1757-899X/252/1/012058.
56. Bernard, P.; Lippert, M. 2015- Nickel–Cadmium and Nickel–Metal Hydride Battery Energy Storage. In *Electrochemical Energy Storage for Renewable Sources and Grid Balancing*; Elsevier, 2015; pp. 223–251 ISBN 978-0-444-62616-5.
57. German, J.M. Hybrid Electric Vehicles. In *Encyclopedia of Energy*; Elsevier, 2004; pp. 197–213 ISBN 978-0-12-176480-7.
58. Tsais, P.-J.; Chan, L.I. 2013- Nickel-Based Batteries: Materials and Chemistry. In *Electricity Transmission, Distribution and Storage Systems*; Elsevier, 2013; pp. 309–397 ISBN 978-1-84569-784-6.
59. Aktaş, A.; Kirçiçek, Y. Solar Hybrid Systems and Energy Storage Systems. In *Solar Hybrid Systems*; Elsevier, 2021; pp. 87–125 ISBN 978-0-323-88499-0.
60. Cao, C.; Steinrück, H.-G. 2023- Molecular-Scale Synchrotron X-Ray Investigations of Solid-Liquid Interfaces in Lithium-Ion Batteries. In *Encyclopedia of Solid-Liquid Interfaces*; Elsevier, 2024; pp. 391–416 ISBN 978-0-323-85670-6.
61. Soto, A.; Berrueta, A.; Mateos, M.; Sanchis, P.; Ursúa, A. 2022- Impact of Micro-Cycles on the Lifetime of Lithium-Ion Batteries: An Experimental Study. *Journal of Energy Storage* **2022**, *55*, 105343. https://doi.org/10.1016/j.est.2022.105343.
62. Keçili, R.; Arli, G.; Hussain, C.M. 2020- Future of Analytical Chemistry with Graphene. In *Comprehensive Analytical Chemistry*; Elsevier, 2020; Vol. 91, pp. 355–389 ISBN 978-0-323-85371-2.
63. Lei, H.; Han, Y.Y. 2019- The Measurement and Analysis for Open Circuit Voltage of Lithium-Ion Battery. *J. Phys.: Conf. Ser.* **2019**, *1325*, 012173. https://doi.org/10.1088/1742-6596/1325/1/012173.
64. Gao, X.; Liu, K.; Su, C.; Zhang, W.; Dai, Y.; Parkin, I.P.; Carmalt, C.J.; He, G. From Bibliometric Analysis: 3D Printing Design Strategies and Battery Applications with a Focus on Zinc-Ion Batteries. *SmartMat* **2024**, *5*, e1197. https://doi.org/10.1002/smm2.1197.
65. Torabi, F.; Ahmadi, P. Battery Technologies. In *Simulation of Battery Systems*; Elsevier, 2020; pp. 1–54 ISBN 978-0-12-816212-5.
66. Delannoy, P.-E.; Riou, B.; Brousse, T.; Le Bideau, J.; Guyomard, D.; Lestriez, B. Ink-Jet Printed Porous Composite LiFePO4 Electrode from Aqueous Suspension for Microbatteries. *Journal of Power Sources* **2015**, *287*, 261–268. https://doi.org/10.1016/j.jpowsour.2015.04.067.
67. Zhou, L.; Ning, W.; Wu, C.; Zhang, D.; Wei, W.; Ma, J.; Li, C.; Chen, L. 3D-Printed Microelectrodes with a Developed Conductive Network and Hierarchical Pores toward High Areal Capacity for Microbatteries. *Advanced Materials Technologies* **2019**, *4*. https://doi.org/10.1002/admt.201800402.
68. Wang, Y.; Chen, C.; Xie, H.; Gao, T.; Yao, Y.; Pastel, G.; Han, X.; Li, Y.; Zhao, J.; Fu, K. (Kelvin); et al. 3D-Printed All-Fiber Li-Ion Battery toward Wearable Energy Storage. *Advanced Functional Materials* **2017**, *27*, 1703140. https://doi.org/10.1002/adfm.201703140.
69. Huang, J.; Yang, J.; Li, W.; Cai, W.; Jiang, Z. Electrochemical Properties of LiCoO2 Thin Film Electrode Prepared by Ink-Jet Printing Technique. *Thin Solid Films* **2008**, *516*, 3314–3319. https://doi.org/10.1016/j.tsf.2007.09.039.

70. Solid State Thin-Film Lithium Battery Systems. *Current Opinion in Solid State and Materials Science* **1999**, *4*, 479–482. https://doi.org/10.1016/S1359-0286(99)00052-2.
71. Schwenzel, J.; Thangadurai, V.; Weppner, W. Developments of High-Voltage All-Solid-State Thin-Film Lithium Ion Batteries. *Journal of Power Sources* **2006**, *154*, 232–238. https://doi.org/10.1016/j.jpowsour.2005.03.223.
72. Clement, B.; Lyu, M.; Sandeep Kulkarni, E.; Lin, T.; Hu, Y.; Lockett, V.; Greig, C.; Wang, L. Recent Advances in Printed Thin-Film Batteries. *Engineering* **2022**, *13*, 238–261. https://doi.org/10.1016/j.eng.2022.04.002.
73. Ding, J.; Shen, K.; Du, Z.; Li, B.; Yang, S. 3D-Printed Hierarchical Porous Frameworks for Sodium Storage. *ACS Appl. Mater. Interfaces* **2017**, *9*, 41871–41877. https://doi.org/10.1021/acsami.7b12892.
74. Additive Manufacturing Enabled, Microarchitected, Hierarchically Porous Polylactic-Acid/Lithium Iron Phosphate/Carbon Nanotube Nanocomposite Electrodes for High Performance Li-Ion Batteries. *Journal of Power Sources* **2021**, *494*, 229625. https://doi.org/10.1016/j.jpowsour.2021.229625.
75. Saleh, M.S.; Li, J.; Park, J.; Panat, R. 3D Printed Hierarchically-Porous Microlattice Electrode Materials for Exceptionally High Specific Capacity and Areal Capacity Lithium Ion Batteries. *Additive Manufacturing* **2018**, *23*, 70–78. https://doi.org/10.1016/j.addma.2018.07.006.
76. Liu, C.; Qiu, Y.; Liu, Y.; Xu, K.; Zhao, N.; Lao, C.; Shen, J.; Chen, Z. Novel 3D Grid Porous Li4Ti5O12 Thick Electrodes Fabricated by 3D Printing for High Performance Lithium-Ion Batteries. *J Adv Ceram* **2022**, *11*, 295–307. https://doi.org/10.1007/s40145-021-0533-7.
77. Liu, C.; Cheng, X.; Li, B.; Chen, Z.; Mi, S.; Lao, C. Fabrication and Characterization of 3D-Printed Highly-Porous 3D LiFePO4 Electrodes by Low Temperature Direct Writing Process. *Materials* **2017**, *10*, 934. https://doi.org/10.3390/ma10080934.
78. Martinez, A.C.; Maurel, A.; Aranzola, A.P.; Grugeon, S.; Panier, S.; Dupont, L.; Hernandez-Viezcas, J.A.; Mummareddy, B.; Armstrong, B.L.; Cortes, P.; et al. Additive Manufacturing of LiNi1/3Mn1/3Co1/3O2 Battery Electrode Material via Vat Photopolymerization Precursor Approach. *Sci Rep* **2022**, *12*, 1–13. https://doi.org/10.1038/s41598-022-22444-1.
79. Yang, Q.; Liu, Q.; Ling, W.; Dai, H.; Chen, H.; Liu, J.; Qiu, Y.; Zhong, L. Porous Electrode Materials for Zn-Ion Batteries: From Fabrication and Electrochemical Application. *Batteries* **2022**, *8*, 223. https://doi.org/10.3390/batteries8110223.
80. Yang, Y.; Ai, L.; Yu, S.; He, J.; Xu, T.; Chen, D.; Shen, L. 3D-Printed Porous GO Framework Enabling Dendrite-Free Lithium-Metal Anodes. *ACS Applied Energy Materials* **2022**. https://doi.org/10.1021/acsaem.2c03267.
81. Chen, C.; Li, S.; Notten, P.H.L.; Zhang, Y.; Hao, Q.; Zhang, X.; Lei, W. 3D Printed Lithium-Metal Full Batteries Based on a High-Performance Three-Dimensional Anode Current Collector. *ACS Appl. Mater. Interfaces* **2021**, *13*, 24785–24794. https://doi.org/10.1021/acsami.1c03997.
82. Zhang, M.; Li, L.; Lin, Q.; Tang, M.; Wu, Y.; Ke, C. Hierarchical-Coassembly-Enabled 3D-Printing of Homogeneous and Heterogeneous Covalent Organic Frameworks. *Journal of the American Chemical Society* **2019**. https://doi.org/10.1021/jacs.9b01561.
83. Mu, Y.; Chu, Y.; Pan, L.; Wu, B.; Zou, L.; He, J.; Han, M.; Zhao, T.; Zeng, L. 3D Printing Critical Materials for Rechargeable Batteries: From Materials, Design and Optimization Strategies to Applications. *Int. J. Extrem. Manuf.* **2023**, *5*, 042008. https://doi.org/10.1088/2631-7990/acf172.
84. Menon, A.; Khan, A.; Balakrishnan, N.T.M.; Raghavan, P.; Leon Y Leon, C.A.; Khan, H.A.; Fatima, M.J.J.; Owuor, P.S. Advances in 3D Printing for Electrochemical Energy Storage Systems. *J. Mater. Sci. Technol. Res.* **2021**, *8*, 50–69. https://doi.org/10.31875/2410-4701.2021.08.7.
85. Thakur, A.R.; Dong, X. Experimental and Numerical Studies of Slurry-Based Coextrusion Deposition of Continuous Carbon Fiber Micro-Batteries to Additively Manufacture 3D Structural Battery Composites. *Composites Part B: Engineering* **2023**, *255*, 110632. https://doi.org/10.1016/j.compositesb.2023.110632.
86. Cheng, M. Direct Ink Writing of Polymer Batteries. Ph.D., University of Illinois at Chicago: United States -- Illinois, 2020.
87. Ragones, H.; Menkin, S.; Kamir, Y.; Gladkikh, A.; Mukra, T.; Kosa, G.; Golodnitsky, D. Towards Smart Free Form-Factor 3D Printable Batteries. *Sustainable Energy & Fuels* **2018**, *2*, 1542–1549. https://doi.org/10.1039/C8SE00122G.
88. Ponnada, S.; Babu Gorle, D.; Chandra Bose, R.S.; Sadat Kiai, M.; Devi, M.; Venkateswara Raju, C.; Baydogan, N.; Kar Nanda, K.; Marken, F.; Sharma, R.K. Current Insight into 3D Printing in Solid-State Lithium-Ion Batteries: A Perspective. *Batteries & Supercaps* **2022**, *5*, e202200223. https://doi.org/10.1002/batt.202200223.

89. Nyika, J.; Mwema, F.M.; Mahamood, R.M.; Akinlabi, E.T.; Jen, T. Advances in 3D Printing Materials Processing-Environmental Impacts and Alleviation Measures. *Advances in Materials and Processing Technologies* **2022**, *8*, 1275–1285. https://doi.org/10.1080/2374068X.2021.1945311.
90. Mao, M.; He, J.; Li, X.; Zhang, B.; Lei, Q.; Liu, Y.; Li, D. The Emerging Frontiers and Applications of High-Resolution 3D Printing. *Micromachines* **2017**, *8*, 113. https://doi.org/10.3390/mi8040113.
91. Park, Y.-G.; Yun, I.; Chung, W.G.; Park, W.; Lee, D.H.; Park, J.-U. High-Resolution 3D Printing for Electronics. *Advanced Science* **2022**, *9*, 2104623. https://doi.org/10.1002/advs.202104623.
92. Ahn, D.; Stevens, L.M.; Zhou, K.; Page, Z.A. Rapid High-Resolution Visible Light 3D Printing. *ACS Central Science* **2020**. https://doi.org/10.1021/acscentsci.0c00929.
93. High-Resolution PLA-Based Composite Scaffolds via 3-D Printing Technology. *Acta Biomaterialia* **2013**, *9*, 5521–5530. https://doi.org/10.1016/j.actbio.2012.10.041.
94. Toward High Resolution 3D Printing of Shape-Conformable Batteries via Vat Photopolymerization: Review and Perspective Available online: https://ieeexplore.ieee.org/abstract/document/9568946/ (accessed on 27 October 2023).
95. Fonseca, N.; Thummalapalli, S.V.; Jambhulkar, S.; Ravichandran, D.; Zhu, Y.; Patil, D.; Thippanna, V.; Ramanathan, A.; Xu, W.; Guo, S.; et al. 3D Printing-Enabled Design and Manufacturing Strategies for Batteries: A Review. *Small* **2023**, 2302718. https://doi.org/10.1002/smll.202302718.
96. Emerging Application of 3D-Printing Techniques in Lithium Batteries: From Liquid to Solid. *Materials Today* **2022**, *59*, 161–181. https://doi.org/10.1016/j.mattod.2022.07.016.
97. 3D Printing for Rechargeable Lithium Metal Batteries. *Energy Storage Materials* **2021**, *38*, 141–156. https://doi.org/10.1016/j.ensm.2021.02.041.
98. Mu, T.; Xiang, L.; Wan, X.; Lou, S.; Du, C.; Zuo, P.; Yin, G. Ultrahigh Areal Capacity Silicon Anodes Realized via Manipulating Electrode Structure. *Energy Storage Materials* **2022**, *53*, 958–968. https://doi.org/10.1016/j.ensm.2022.10.021.
99. Zhang, M.; Mei, H.; Chang, P.; Cheng, L. 3D Printing of Structured Electrodes for Rechargeable Batteries. *J. Mater. Chem. A* **2020**, *8*, 10670–10694. https://doi.org/10.1039/D0TA02099K.
100. Lyu, Z.; Lim, G.J.H.; Guo, R.; Kou, Z.; Wang, T.; Guan, C.; Ding, J.; Chen, W.; Wang, J. 3D-Printed MOF-Derived Hierarchically Porous Frameworks for Practical High-Energy Density Li–O2 Batteries. *Advanced Functional Materials* **2019**, *29*, 1806658. https://doi.org/10.1002/adfm.201806658.
101. Gao, X.; Yang, X.; Wang, S.; Sun, Q.; Zhao, C.; Li, X.; Liang, J.; Zheng, M.; Zhao, Y.; Wang, J.; et al. A 3D-Printed Ultra-High Se Loading Cathode for High Energy Density Quasi-Solid-State Li–Se Batteries. *Journal of Materials Chemistry A* **2020**, *8*, 278–286. https://doi.org/10.1039/C9TA10623E.
102. All 3D Printing Lithium Metal Batteries with Hierarchically and Conductively Porous Skeleton for Ultrahigh Areal Energy Density. *Energy Storage Materials* **2023**, *54*, 304–312. https://doi.org/10.1016/j.ensm.2022.10.036.
103. 3D Printing of Fast Kinetics Reconciled Ultra-Thick Cathodes for High Areal Energy Density Aqueous Li–Zn Hybrid Battery. *Science Bulletin* **2022**, *67*, 1253–1263. https://doi.org/10.1016/j.scib.2022.04.015.
104. Wang, J.; Sun, Q.; Gao, X.; Wang, C.; Li, W.; Holness, F.B.; Zheng, M.; Li, R.; Price, A.D.; Sun, X.; et al. Toward High Areal Energy and Power Density Electrode for Li-Ion Batteries via Optimized 3D Printing Approach. *ACS Appl. Mater. Interfaces* **2018**, *10*, 39794–39801. https://doi.org/10.1021/acsami.8b14797.
105. Marschewski, J.; Brenner, L.; Ebejer, N.; Ruch, P.; Michel, B.; Poulikakos, D. 3D-Printed Fluidic Networks for High-Power-Density Heat-Managing Miniaturized Redox Flow Batteries. *Energy & Environmental Science* **2017**, *10*, 780–787. https://doi.org/10.1039/C6EE03192G.
106. Li, J.; Du, Z.; Ruther, R.E.; An, S.J.; David, L.A.; Hays, K.; Wood, M.; Phillip, N.D.; Sheng, Y.; Mao, C.; et al. Toward Low-Cost, High-Energy Density, and High-Power Density Lithium-Ion Batteries. *JOM* **2017**, *69*, 1484–1496. https://doi.org/10.1007/s11837-017-2404-9.
107. Wei, T.-S.; Ahn, B.Y.; Grotto, J.; Lewis, J.A. 3D Printing of Customized Li-Ion Batteries with Thick Electrodes. *Advanced Materials* **2018**, *30*, 1703027. https://doi.org/10.1002/adma.201703027.
108. Shi, H.; Cao, J.; Sun, Z.; Ghazi, Z.A.; Zhu, X.; Han, S.; Ren, D.; Lu, G.; Lan, H.; Li, F. 3D Printing Enables Customizable Batteries. *Batteries & Supercaps* **2023**, *6*, e202300161. https://doi.org/10.1002/batt.202300161.
109. Design and Fabrication of Multifunctional Structural Batteries. *Journal of Power Sources* **2009**, *189*, 646–650. https://doi.org/10.1016/j.jpowsour.2008.09.082.
110. Robust Free-Standing Electrodes for Flexible Lithium-Ion Batteries Prepared by a Conventional Electrode Fabrication Process. *Electrochimica Acta* **2017**, *247*, 371–380. https://doi.org/10.1016/j.electacta.2017.07.032.

111. Roberts, M.; Johns, P.; Owen, J.; Brandell, D.; Edstrom, K.; Enany, G.E.; Guery, C.; Golodnitsky, D.; Lacey, M.; Lecoeur, C.; et al. 3D Lithium Ion Batteries—from Fundamentals to Fabrication. *Journal of Materials Chemistry* **2011**, *21*, 9876–9890. https://doi.org/10.1039/C0JM04396F.
112. Hao, F.; Han, F.; Liang, Y.; Wang, C.; Yao, Y. Architectural Design and Fabrication Approaches for Solid-State Batteries. *MRS Bulletin* **2018**, *43*, 775–781. https://doi.org/10.1557/mrs.2018.211.
113. Bhosale, V.S.; Gaikwad, P.M.; Maladkar, N.P.; Desai, K.V. A Review on Use of 3D Printing for Battery Manufacturing. **2022**.
114. Comprehensive Review on Various Additive Manufacturing Techniques and Its Implementation in Electronic Devices. *Journal of Manufacturing Systems* **2022**, *62*, 477–502. https://doi.org/10.1016/j.jmsy.2022.01.002.
115. Bates, A.M.; Preger, Y.; Torres-Castro, L.; Harrison, K.L.; Harris, S.J.; Hewson, J. Are Solid-State Batteries Safer than Lithium-Ion Batteries? *Joule* **2022**, *6*, 742–755. https://doi.org/10.1016/j.joule.2022.02.007.
116. He, Y.; Chen, S.; Nie, L.; Sun, Z.; Wu, X.; Liu, W. Stereolithography Three-Dimensional Printing Solid Polymer Electrolytes for All-Solid-State Lithium Metal Batteries. *Nano Lett.* **2020**, *20*, 7136–7143. https://doi.org/10.1021/acs.nanolett.0c02457.
117. Zekoll, S.; Marriner-Edwards, C.; Hekselman, A.K.O.; Kasemchainan, J.; Kuss, C.; Armstrong, D.E.J.; Cai, D.; Wallace, R.J.; Richter, F.H.; Thijssen, J.H.J.; et al. Hybrid Electrolytes with 3D Bicontinuous Ordered Ceramic and Polymer Microchannels for All-Solid-State Batteries. *Energy Environ. Sci.* **2018**, *11*, 185–201. https://doi.org/10.1039/C7EE02723K.
118. Processing and Manufacturing of next Generation Lithium-Based All Solid-State Batteries. *Current Opinion in Solid State and Materials Science* **2022**, *26*, 101003. https://doi.org/10.1016/j.cossms.2022.101003.
119. Schnell, J.; Tietz, F.; Singer, C.; Hofer, A.; Billot, N.; Reinhart, G. Prospects of Production Technologies and Manufacturing Costs of Oxide-Based All-Solid-State Lithium Batteries. *Energy & Environmental Science* **2019**, *12*, 1818–1833. https://doi.org/10.1039/C8EE02692K.
120. Li, H.; Liang, J. Recent Development of Printed Micro-Supercapacitors: Printable Materials, Printing Technologies, and Perspectives. *Adv. Mater.* **2020**, *32*, 1805864. https://doi.org/10.1002/adma.201805864.
121. Lin, Y.; Gao, Y.; Fang, F.; Fan, Z. Recent Progress on Printable Power Supply Devices and Systems with Nanomaterials. *Nano Res.* **2018**, *11*, 3065–3087. https://doi.org/10.1007/s12274-018-2068-y.
122. Ma, J.; Zheng, S.; Chi, L.; Liu, Y.; Zhang, Y.; Wang, K.; Wu, Z.-S. 3D Printing Flexible Sodium-Ion Microbatteries with Ultrahigh Areal Capacity and Robust Rate Capability. *Advanced Materials* **2022**, *34*, 2205569. https://doi.org/10.1002/adma.202205569.
123. Thermal Management of Lithium-Ion Battery Cells Using 3D Printed Phase Change Composites. *Applied Thermal Engineering* **2020**, *171*, 115126. https://doi.org/10.1016/j.applthermaleng.2020.115126.
124. 3D Printed Separator for the Thermal Management of High-Performance Li Metal Anodes. *Energy Storage Materials* **2018**, *12*, 197–203. https://doi.org/10.1016/j.ensm.2017.12.019.
125. Lewis, J.A. Direct Ink Writing of 3D Functional Materials. *Adv. Funct. Mater.* **2006**, *16*, 2193–2204. https://doi.org/10.1002/adfm.200600434.
126. Tagliaferri, S.; Panagiotopoulos, A.; Mattevi, C. Direct Ink Writing of Energy Materials. *Materials Advances* **2021**, *2*, 540–563. https://doi.org/10.1039/D0MA00753F.
127. Saadi, M. a. S.R.; Maguire, A.; Pottackal, N.T.; Thakur, M.S.H.; Ikram, M.M.; Hart, A.J.; Ajayan, P.M.; Rahman, M.M. Direct Ink Writing: A 3D Printing Technology for Diverse Materials. *Advanced Materials* **2022**, *34*, 2108855. https://doi.org/10.1002/adma.202108855.
128. High-Precision Resistance Strain Sensors of Multilayer Composite Structure via Direct Ink Writing: Optimized Layer Flatness and Interfacial Strength. *Composites Science and Technology* **2021**, *201*, 108530. https://doi.org/10.1016/j.compscitech.2020.108530.
129. Chen, B.; Willenbacher, N. High-Precision Direct Ink Writing of Li6.4La3Zr1.4Ta0.6O12. *Journal of the European Ceramic Society* **2022**, *42*, 7491–7500. https://doi.org/10.1016/j.jeurceramsoc.2022.09.018.
130. Loaldi, D.; Piccolo, L.; Brown, E.; Tosello, G.; Shemelya, C.; Masato, D. Hybrid Process Chain for the Integration of Direct Ink Writing and Polymer Injection Molding. *Micromachines* **2020**, *11*. https://doi.org/10.3390/mi11050509.
131. Yuk, H.; Zhao, X. A New 3D Printing Strategy by Harnessing Deformation, Instability, and Fracture of Viscoelastic Inks. *Advanced Materials* **2017**, *30*. https://doi.org/10.1002/adma.201704028.

132. Rocha, V.G.; Saiz, E.; Tirichenko, I.S.; García-Tuñón, E. Direct Ink Writing Advances in Multi-Material Structures for a Sustainable Future. *J. Mater. Chem. A* **2020**, *8*, 15646–15657. https://doi.org/10.1039/D0TA04181E.
133. Yirmibesoglu, O.D.; Simonsen, L.E.; Manson, R.; Davidson, J.; Healy, K.; Menguc, Y.; Wallin, T. Multi-Material Direct Ink Writing of Photocurable Elastomeric Foams. *Commun Mater* **2021**, *2*, 1–14. https://doi.org/10.1038/s43246-021-00186-3.
134. Xu, C.; Quinn, B.; Lebel, L.L.; Therriault, D.; L'Espérance, G. Multi-Material Direct Ink Writing (DIW) for Complex 3D Metallic Structures with Removable Supports. *ACS Appl. Mater. Interfaces* **2019**, *11*, 8499–8506. https://doi.org/10.1021/acsami.8b19986.
135. Renteria, A.; Balcorta, V.H.; Marquez, C.; Rodriguez, A.A.; Renteria-Marquez, I.; Regis, J.; Wilburn, B.; Patterson, S.; Espalin, D.; Tseng, T.-L. (Bill); et al. Direct Ink Write Multi-Material Printing of PDMS-BTO Composites with MWCNT Electrodes for Flexible Force Sensors. *Flex. Print. Electron.* **2022**, *7*, 015001. https://doi.org/10.1088/2058-8585/ac442e.
136. Cadiou, T.; Demoly, F.; Gomes, S. A Hybrid Additive Manufacturing Platform Based on Fused Filament Fabrication and Direct Ink Writing Techniques for Multi-Material 3D Printing. *Int J Adv Manuf Technol* **2021**, *114*, 3551–3562. https://doi.org/10.1007/s00170-021-06891-0.
137. Mantelli, A.; Romani, A.; Suriano, R.; Levi, M.; Turri, S. Direct Ink Writing of Recycled Composites with Complex Shapes: Process Parameters and Ink Optimization. *Advanced Engineering Materials* **2021**, *23*. https://doi.org/10.1002/adem.202100116.
138. Wei, M.; Zhang, F.; Wang, W.; Alexandridis, P.; Zhou, C.; Wu, G. 3D Direct Writing Fabrication of Electrodes for Electrochemical Storage Devices. *Journal of Power Sources* **2017**, *354*. https://doi.org/10.1016/j.jpowsour.2017.04.042.
139. Li, Q.; Dong, Q.; Wang, J.; Xue, Z.; Li, J.; Yu, M.; Zhang, T.; Wan, Y.; Sun, H. Direct Ink Writing (DIW) of Graphene Aerogel Composite Electrode for Vanadium Redox Flow Battery. *Journal of Power Sources* **2022**, *542*, 231810. https://doi.org/10.1016/j.jpowsour.2022.231810.
140. Zhu, C.; Schorr, N.B.; Qi, Z.; Wygant, B.R.; Turney, D.E.; Yadav, G.G.; Worsley, M.A.; Duoss, E.B.; Banerjee, S.; Spoerke, E.D.; et al. Direct Ink Writing of 3D Zn Structures as High-Capacity Anodes for Rechargeable Alkaline Batteries. *Small Structures* **2023**, *4*, 2200323. https://doi.org/10.1002/sstr.202200323.
141. Liu, Z.; Tian, X.; Liu, M.; Duan, S.; Ren, Y.; Ma, H.; Tang, K.; Shi, J.; Hou, S.; Jin, H.; et al. Direct Ink Writing of $Li_{1.3}Al_{0.3}Ti_{1.7}(PO_4)_3$ -Based Solid-State Electrolytes with Customized Shapes and Remarkable Electrochemical Behaviors. *Small* **2021**, *17*, 2002866. https://doi.org/10.1002/smll.202002866.
142. Tao, R.; Gu, Y.; Sharma, J.; Hong, K.; Li, J. A Conformal Heat-Drying Direct Ink Writing 3D Printing for High-Performance Lithium-Ion Batteries. *Materials Today Chemistry* **2023**, *32*, 101672. https://doi.org/10.1016/j.mtchem.2023.101672.
143. Li, L.; Tan, H.; Yuan, X.; Ma, H.; Ma, Z.; Zhao, Y.; Zhao, J.; Wang, X.; Chen, D.; Dong, Y. Direct Ink Writing Preparation of LiFePO4/MWCNTs Electrodes with High-Areal Li-Ion Capacity. *Ceramics International* **2021**, *47*, 21161–21166. https://doi.org/10.1016/j.ceramint.2021.04.119.
144. Rasul, M.G.; Cheng, M.; Jiang, Y.; Pan, Y.; Shahbazian-Yassar, R. Direct Ink Printing of PVdF Composite Polymer Electrolytes with Aligned BN Nanosheets for Lithium-Metal Batteries. *ACS Nanosci. Au* **2022**, acsnanoscienceau.1c00056. https://doi.org/10.1021/acsnanoscienceau.1c00056.
145. Liu, C.; Zhao, N.; Xu, K.; Li, Y.; Mwizerwa, J.P.; Shen, J.; Chen, Z. High-Performance LiFePO4 and SiO@C/Graphite Interdigitated Full Lithium-Ion Battery Fabricated via Low Temperature Direct Write 3D Printing. *Materials Today Energy* **2022**, *29*, 101098. https://doi.org/10.1016/j.mtener.2022.101098.
146. FDM vs. FFF: Differences and Comparison Available online: https://www.xometry.com/resources/3d-printing/fdm-vs-fff-3d-printing/ (accessed on 24 January 2024).
147. Jones, R.; Haufe, P.; Sells, E.; Iravani, P.; Olliver, V.; Palmer, C.; Bowyer, A. RepRap – the Replicating Rapid Prototyper. *Robotica* **2011**, *29*, 177–191. https://doi.org/10.1017/S026357471000069X.
148. Sells, E.; Bailard, S.; Smith, Z.; Bowyer, A.; Olliver, V. RepRap: The Replicating Rapid Prototyper: Maximizing Customizability by Breeding the Means of Production. In *Handbook of Research in Mass Customization and Personalization*; World Scientific Publishing Company, 2009; pp. 568–580 ISBN 978-981-4280-25-9.
149. Bowyer, A. 3D Printing and Humanity's First Imperfect Replicator. *3D Printing and Additive Manufacturing* **2014**, *1*, 4–5. https://doi.org/10.1089/3dp.2013.0003.

150. Reyes, C.; Somogyi, R.; Niu, S.; Cruz, M.A.; Yang, F.; Catenacci, M.J.; Rhodes, C.P.; Wiley, B.J. Three-Dimensional Printing of a Complete Lithium Ion Battery with Fused Filament Fabrication. *ACS Appl. Energy Mater.* **2018**, acsaem.8b00885. https://doi.org/10.1021/acsaem.8b00885.
151. 3D Printing a Complete Lithium Ion Battery with Fused Filament Fabrication | Request PDF Available online: https://www.researchgate.net/publication/327735139_3D_Printing_a_Complete_Lithium_Ion_Battery_with_Fused_Filament_Fabrication (accessed on 2 November 2023).
152. Mecheter, A.; Tarlochan, F. Fused Filament Fabrication Three-Dimensional Printing: Assessing the Influence of Geometric Complexity and Process Parameters on Energy and the Environment. *Sustainability* **2023**, *15*, 12319. https://doi.org/10.3390/su151612319.
153. Sola, A. Materials Requirements in Fused Filament Fabrication: A Framework for the Design of Next-Generation 3D Printable Thermoplastics and Composites. *Macromolecular Materials and Engineering* **2022**, *307*, 2200197. https://doi.org/10.1002/mame.202200197.
154. Maurel, A.; Courty, M.; Fleutot, B.; Tortajada, H.; Prashantha, K.; Armand, M.; Grugeon, S.; Panier, S.; Dupont, L. Highly Loaded Graphite–Polylactic Acid Composite-Based Filaments for Lithium-Ion Battery Three-Dimensional Printing. *Chem. Mater.* **2018**, *30*, 7484–7493. https://doi.org/10.1021/acs.chemmater.8b02062.
155. Baechler, C.; DeVuono, M.; Pearce, J.M. Distributed Recycling of Waste Polymer into RepRap Feedstock. *Rapid Prototyping Journal* **2013**, *19*, 118–125. https://doi.org/10.1108/13552541311302978.
156. Cruz Sanchez, F.A.; Boudaoud, H.; Hoppe, S.; Camargo, M. Polymer Recycling in an Open-Source Additive Manufacturing Context: Mechanical Issues. *Additive Manufacturing* **2017**, *17*, 87–105. https://doi.org/10.1016/j.addma.2017.05.013.
157. Cruz Sanchez, F.A.; Boudaoud, H.; Camargo, M.; Pearce, J.M. Plastic Recycling in Additive Manufacturing: A Systematic Literature Review and Opportunities for the Circular Economy. *Journal of Cleaner Production* **2020**, *264*, 121602. https://doi.org/10.1016/j.jclepro.2020.121602.
158. Dertinger, S.C.; Gallup, N.; Tanikella, N.G.; Grasso, M.; Vahid, S.; Foot, P.J.S.; Pearce, J.M. Technical Pathways for Distributed Recycling of Polymer Composites for Distributed Manufacturing: Windshield Wiper Blades. *Resources, Conservation and Recycling* **2020**, *157*, 104810. https://doi.org/10.1016/j.resconrec.2020.104810.
159. Fully Metallic Copper 3D-Printed Electrodes via Sintering for Electrocatalytic Biosensing. *Applied Materials Today* **2021**, *25*, 101253. https://doi.org/10.1016/j.apmt.2021.101253.
160. Mo, F.; Guo, B.; Liu, Q.; Ling, W.; Liang, G.; Chen, L.; Yu, S.; Wei, J. Additive Manufacturing for Advanced Rechargeable Lithium Batteries: A Mini Review. *Front. Energy Res.* **2022**, *10*, 986985. https://doi.org/10.3389/fenrg.2022.986985.
161. Chen, Y.; Liu, Y.; Chen, J.; Wang, Z.; Tang, B. Hybrid Energy Storage System Design for Mobile Multi-Material Fused Deposition Modeling. *AIP Advances* **2020**, *10*, 075322. https://doi.org/10.1063/5.0014097.
162. Anzalone, G.C.; Wijnen, B.; Pearce, J.M. Multi-Material Additive and Subtractive Prosumer Digital Fabrication with a Free and Open-Source Convertible Delta RepRap 3-D Printer. *Rapid Prototyping Journal* **2015**, *21*, 506–519. https://doi.org/10.1108/RPJ-09-2014-0113.
163. Nanomaterials-Based Additive Manufacturing for Mass Production of Energy Storage Systems: 3D Printed Batteries and Supercapacitors.
164. Maurel, A. Thermoplastic Composite Filaments Formulation and 3D-Printing of a Lithium-Ion Battery via Fused Deposition Modeling. phdthesis, Université de Picardie Jules Verne, 2020.
165. Challenges of 3D Printing in LIB Electrodes: Emphasis on Material-Design Properties, and Performance of 3D Printed Si-Based LIB Electrodes. *Journal of Power Sources* **2022**, *543*, 231840. https://doi.org/10.1016/j.jpowsour.2022.231840.
166. Laureto, J.J.; Pearce, J.M. Anisotropic Mechanical Property Variance between ASTM D638-14 Type i and Type Iv Fused Filament Fabricated Specimens. *Polymer Testing* **2018**, *68*, 294–301. https://doi.org/10.1016/j.polymertesting.2018.04.029.
167. Fused Filament Fabrication of Polymer Materials: A Review of Interlayer Bond. *Additive Manufacturing* **2021**, *37*, 101658. https://doi.org/10.1016/j.addma.2020.101658.
168. Beydaghi, H.; Abouali, S.; Thorat, S.B.; Del Rio Castillo, A.E.; Bellani, S.; Lauciello, S.; Gentiluomo, S.; Pellegrini, V.; Bonaccorso, F. 3D Printed Silicon-Few Layer Graphene Anode for Advanced Li-Ion Batteries. *RSC Adv.* **2021**, *11*, 35051–35060. https://doi.org/10.1039/D1RA06643A.

169. Maurel, A.; Grugeon, S.; Fleutot, B.; Courty, M.; Prashantha, K.; Tortajada, H.; Armand, M.; Panier, S.; Dupont, L. Three-Dimensional Printing of a LiFePO4/Graphite Battery Cell via Fused Deposition Modeling. *Sci Rep* **2019**, *9*, 18031. https://doi.org/10.1038/s41598-019-54518-y.
170. Gao, W.; Michalička, J.; Pumera, M. Hierarchical Atomic Layer Deposited V_2O_5 on 3D Printed Nanocarbon Electrodes for High-Performance Aqueous Zinc-Ion Batteries. *Small* **2022**, *18*, 2105572. https://doi.org/10.1002/smll.202105572.
171. Foster, C.W.; Zou, G.; Jiang, Y.; Down, M.P.; Liauw, C.M.; Garcia-Miranda Ferrari, A.; Ji, X.; Smith, G.C.; Kelly, P.J.; Banks, C.E. Next-Generation Additive Manufacturing: Tailorable Graphene/Polylactic(Acid) Filaments Allow the Fabrication of 3D Printable Porous Anodes for Utilisation within Lithium-Ion Batteries. *Batteries & Supercaps* **2019**, *2*, 448–453. https://doi.org/10.1002/batt.201800148.
172. Hu, X.; Chen, Y.; Xu, W.; Zhu, Y.; Kim, D.; Fan, Y.; Yu, B.; Chen, Y. 3D-Printed Thermoplastic Polyurethane Electrodes for Customizable, Flexible Lithium-Ion Batteries with an Ultra-Long Lifetime. *Small* **2023**, *19*, 2301604. https://doi.org/10.1002/smll.202301604.
173. Maurel, A.; Armand, M.; Grugeon, S.; Fleutot, B.; Davoisne, C.; Tortajada, H.; Courty, M.; Panier, S.; Dupont, L. Poly(Ethylene Oxide)−LiTFSI Solid Polymer Electrolyte Filaments for Fused Deposition Modeling Three-Dimensional Printing. *J. Electrochem. Soc.* **2020**, *167*, 070536. https://doi.org/10.1149/1945-7111/ab7c38.
174. Yang, P.; Fan, H.J. Inkjet and Extrusion Printing for Electrochemical Energy Storage: A Minireview. *Advanced Materials Technologies* **2020**, *5*, 2000217. https://doi.org/10.1002/admt.202000217.
175. Sousa, R.E.; Costa, C.M.; Lanceros-Méndez, S. Advances and Future Challenges in Printed Batteries. *ChemSusChem* **2015**, *8*, 3539–3555. https://doi.org/10.1002/cssc.201500657.
176. Fabrication of Modern Lithium Ion Batteries by 3D Inkjet Printing: Opportunities and Challenges. *Heliyon* **2022**, *8*, e12623. https://doi.org/10.1016/j.heliyon.2022.e12623.
177. Sowade, E.; Polomoshnov, M.; Willert, A.; Baumann, R.R. Toward 3D-Printed Electronics: Inkjet-Printed Vertical Metal Wire Interconnects and Screen-Printed Batteries. *Advanced Engineering Materials* **2019**, *21*, 1900568. https://doi.org/10.1002/adem.201900568.
178. Zhao, Y.; Zhou, Q.; Liu, L.; Xu, J.; Yan, M.; Jiang, Z. A Novel and Facile Route of Ink-Jet Printing to Thin Film SnO2 Anode for Rechargeable Lithium Ion Batteries. *Electrochimica Acta* **2006**, *51*, 2639–2645. https://doi.org/10.1016/j.electacta.2005.07.050.
179. Lawes, S.; Sun, Q.; Lushington, A.; Xiao, B.; Liu, Y.; Sun, X. Inkjet-Printed Silicon as High Performance Anodes for Li-Ion Batteries. *Nano Energy* **2017**, *36*, 313–321. https://doi.org/10.1016/j.nanoen.2017.04.041.
180. Chen, T.; Wang, Y.; Yang, Y.; Huang, F.; Zhu, M.; Ang, B.T.W.; Xue, J.M. Heterometallic Seed-Mediated Zinc Deposition on Inkjet Printed Silver Nanoparticles Toward Foldable and Heat-Resistant Zinc Batteries. *Advanced Functional Materials* **2021**, *31*, 2101607. https://doi.org/10.1002/adfm.202101607.
181. Kushwaha, A.; Jangid, M.K.; Bhatt, B.B.; Mukhopadhyay, A.; Gupta, D. Inkjet-Printed Environmentally Friendly Graphene Film for Application as a High-Performance Anode in Li-Ion Batteries. *ACS Appl. Energy Mater.* **2021**, *4*, 7911–7921. https://doi.org/10.1021/acsaem.1c01249.
182. Kushwaha, A.; Sharma, A.; Bhatt, B.B.; Mukhopadhyay, A.; Gupta, D. Inkjet-Printed Graphene-Modified Aluminum Current Collector for High-Voltage Lithium-Ion Battery. *ACS Appl. Energy Mater.* **2023**, *6*, 4168–4178. https://doi.org/10.1021/acsaem.2c03870.
183. Viviani, P.; Gibertini, E.; Iervolino, F.; Levi, M.; Magagnin, L. Carbon Additive Effect on the Electrochemical Performances of Inkjet Printed Thin-Film Li4Ti5O12 Electrodes. *Journal of Manufacturing Processes* **2021**, *72*, 411–418. https://doi.org/10.1016/j.jmapro.2021.10.039.
184. Kolchanov, D.S.; Mitrofanov, I.; Kim, A.; Koshtyal, Y.; Rumyantsev, A.; Sergeeva, E.; Vinogradov, A.; Popovich, A.; Maximov, M.Yu. Inkjet Printing of Li-Rich Cathode Material for Thin-Film Lithium-Ion Microbatteries. *Energy Technology* **2020**, *8*, 1901086. https://doi.org/10.1002/ente.201901086.
185. Pei, M.; Shi, H.; Yao, F.; Liang, S.; Xu, Z.; Pei, X.; Wang, S.; Hu, Y. 3D Printing of Advanced Lithium Batteries: A Designing Strategy of Electrode/Electrolyte Architectures. *J. Mater. Chem. A* **2021**, *9*, 25237–25257. https://doi.org/10.1039/D1TA06683H.
186. Overview on the Applications of Three-Dimensional Printing for Rechargeable Lithium-Ion Batteries. *Applied Energy* **2020**, *257*, 114002. https://doi.org/10.1016/j.apenergy.2019.114002.
187. Tian, X.; Zhou, K. 3D Printing of Cellular Materials for Advanced Electrochemical Energy Storage and Conversion. *Nanoscale* **2020**, *12*, 7416–7432. https://doi.org/10.1039/D0NR00291G.
188. Narita, K.; Saccone, M.A.; Sun, Y.; Greer, J.R. Additive Manufacturing of 3D Batteries: A Perspective. *Journal of Materials Research* **2022**, *37*, 1535–1546. https://doi.org/10.1557/s43578-022-00562-w.

189. Recent Advances in 3D Printed Electrode Materials for Electrochemical Energy Storage Devices. *Journal of Energy Chemistry* **2023**, *81*, 272–312. https://doi.org/10.1016/j.jechem.2023.01.037.
190. Cheng, M.; Deivanayagam, R.; Shahbazian-Yassar, R. 3D Printing of Electrochemical Energy Storage Devices: A Review of Printing Techniques and Electrode/Electrolyte Architectures. *Batteries & Supercaps* **2020**, *3*, 130–146. https://doi.org/10.1002/batt.201900130.
191. A Comprehensive Review of the Photopolymerization of Ceramic Resins Used in Stereolithography. *Additive Manufacturing* **2020**, *35*, 101177. https://doi.org/10.1016/j.addma.2020.101177.
192. Brinckmann, S.A.; Patra, N.; Yao, J.; Ware, T.H.; Frick, C.P.; Fertig, R.S. Stereolithography of SiOC Polymer-Derived Ceramics Filled with SiC Micronwhiskers. *Advanced Engineering Materials* **2018**, *20*, 1800593. https://doi.org/10.1002/adem.201800593.
193. Chen, Q.; Xu, R.; He, Z.; Zhao, K.; Pan, L. Printing 3D Gel Polymer Electrolyte in Lithium-Ion Microbattery Using Stereolithography. *J. Electrochem. Soc.* **2017**, *164*, A1852–A1857. https://doi.org/10.1149/2.0651709jes.
194. Norjeli, M.F.; Tamchek, N.; Osman, Z.; Mohd Noor, I.S.; Kufian, M.Z.; Ghazali, M.I.B.M. Additive Manufacturing Polyurethane Acrylate via Stereolithography for 3D Structure Polymer Electrolyte Application. *Gels* **2022**, *8*, 589. https://doi.org/10.3390/gels8090589.
195. Lee, K.; Shang, Y.; Bobrin, V.A.; Kuchel, R.; Kundu, D.; Corrigan, N.; Boyer, C. 3D Printing Nanostructured Solid Polymer Electrolytes with High Modulus and Conductivity. *Advanced Materials* **2022**, *34*, 2204816. https://doi.org/10.1002/adma.202204816.
196. Katsuyama, Y.; Kudo, A.; Kobayashi, H.; Han, J.; Chen, M.; Honma, I.; Kaner, R.B. A 3D-Printed, Freestanding Carbon Lattice for Sodium Ion Batteries. *Small* **2022**, *18*, 2202277. https://doi.org/10.1002/smll.202202277.
197. Ye, X.; Wang, C.; Wang, L.; Lu, B.; Gao, F.; Shao, D. DLP Printing of a Flexible Micropattern Si/PEDOT:PSS/PEG Electrode for Lithium-Ion Batteries. *Chem. Commun.* **2022**, *58*, 7642–7645. https://doi.org/10.1039/D2CC01626E.
198. Yoko, A.; Oshima, Y. Recovery of Silicon from Silicon Sludge Using Supercritical Water. *The Journal of Supercritical Fluids* **2013**, *75*, 1–5. https://doi.org/10.1016/j.supflu.2012.12.019.
199. Sun, L.; Liu, Y.; Wu, J.; Shao, R.; Jiang, R.; Tie, Z.; Jin, Z. A Review on Recent Advances for Boosting Initial Coulombic Efficiency of Silicon Anodic Lithium Ion Batteries. *Small* **2022**, *18*, 2102894. https://doi.org/10.1002/smll.202102894.
200. Pearce, J.M. Economic Savings for Scientific Free and Open Source Technology: A Review. *HardwareX* **2020**, *8*, e00139. https://doi.org/10.1016/j.ohx.2020.e00139.
201. Dobbelaere, T.; Vereecken, P.M.; Detavernier, C. A USB-Controlled Potentiostat/Galvanostat for Thin-Film Battery Characterization. *HardwareX* **2017**, *2*, 34–49. https://doi.org/10.1016/j.ohx.2017.08.001.
202. Sylvestrin, G.R.; Scherer, H.F.; Hideo Ando Junior, O. Hardware and Software Development of an Open Source Battery Management System. *IEEE Latin America Transactions* **2021**, *19*, 1153–1163. https://doi.org/10.1109/TLA.2021.9461844.
203. Fleming, J.; Amietszajew, T.; McTurk, E.; Towers, D.P.; Greenwood, D.; Bhagat, R. Development and Evaluation of In-Situ Instrumentation for Cylindrical Li-Ion Cells Using Fibre Optic Sensors. *HardwareX* **2018**, *3*, 100–109. https://doi.org/10.1016/j.ohx.2018.04.001.
204. Carloni, A.; Baronti, F.; Di Rienzo, R.; Roncella, R.; Saletti, R. An Open-Hardware and Low-Cost Maintenance Tool for Light-Electric-Vehicle Batteries. *Energies* **2021**, *14*, 4962. https://doi.org/10.3390/en14164962.
205. Yensen, N.; Allen, P.B. Open Source All-Iron Battery for Renewable Energy Storage. *HardwareX* **2019**, *6*, e00072. https://doi.org/10.1016/j.ohx.2019.e00072.
206. Koirala, D.; Yensen, N.; Allen, P.B. Open Source All-Iron Battery 2.0. *HardwareX* **2021**, *9*, e00171. https://doi.org/10.1016/j.ohx.2020.e00171.